Plant Physiology Preview. Published on April 12, 2011, as DOI:10.1104/pp.111.174334

Running title: Function of *Bphi008a* in Rice

Corresponding author: Guangcun He

Address: College of Life Sciences, Wuhan University, Wuhan 430072, People's Republic of China.

Tel: 86-27-68752384; Fax: 86-27-68752327;

E-mail: gche@whu.edu.cn

Research categories: Signal Transduction and Hormone Action; System Biology, Molecular Biology, and Gene Regulation; Plant Interacting with Other Organisms.

The *Bphi008a* Gene Interacts with the Ethylene Pathway and Transcriptionally Regulates *MAPK* Genes in the Response of Rice to Brown Planthopper Feeding

Jing Hu[1], Jiangbo Zhou[1], Xinxin Peng[1], Henghao Xu[1], Caixiang Liu[1], Bo Du[1], Hongyu Yuan[2], Lili Zhu[1], Guangcun He[1,*]

[1] State Key Laboratory of Hybrid Rice, College of Life Sciences, Wuhan University, Wuhan 430072, People's Republic of China, [2]College of Life Sciences, Xinyang Normal University, Xinyang 464000, People's Republic of China

ABSTRACT

We examined ways in which the *Bphi008a* (AY256682) gene of rice (*Oryza sativa* L.) enhances the plant's resistance to a specialist herbivore, the brown planthopper (*Nilaparvata lugens* Stål; BPH). Measurement of the expression levels of ethylene synthases and of ethylene emissions showed that BPH-feeding rapidly initiated the ethylene signaling pathway and upregulated *Bphi008a* transcript levels after 6-96 h of feeding. In contrast, blocking ethylene transduction (using 1-methylcyclopropene) reduced *Bphi008a* transcript levels in WT plants fed upon by BPH. *In vitro* kinase assays showed that Bphi008a can be phosphorylated by OsMPK5, and yeast two-hybrid assays demonstrated that the C-terminal proline-rich region of Bphi008a interacts directly with this kinase. Furthermore, bimolecular fluorescence complementation (BiFC) assays showed that this interaction occurs in the nucleus. Subsequently, we found that *Bphi008a* up-regulation and down-regulation were accompanied by different changes in transcription levels of *OsMPK5, OsMPK12, OsMPK13* and *OsMPK17* in transgenic plants. Immunoblot analysis also showed that the OsMPK5 protein level increased in over-expressing plants and decreased in RNAi plants after BPH-feeding. In transgenic lines, changes in the expression levels of several enzymes that are important components of the defenses against the BPH were also observed. Finally, yeast two-hybrid screening results showed that Bphi008a is able to interact with a b-ZIP transcription factor (OsbZIP60) and a RNA polymerase polypeptide (SDRP).

INTRODUCTION

Plants are sessile and constantly exposed to diverse external biotic stresses during their life cycle (e.g., viruses, pathogens and pest infestations). Plant defenses to external biotic stresses differ from those of mammals, which have evolved specialized mobile defense lymphocytes and a somatic acquired immune system that provide protection against external stimuli. Instead, plants depend on a pre-existing innate immune system in each cell (Ausubel, 2005). The innate immunity of plants can provide them with non-host resistance and host-resistance against external biotic stresses. In addition, mutant and transcription analyses have shown that several low molecular weight signal molecules, including salicylic acid (SA), jasmonic acid (JA) and ethylene (Et), play important roles in the regulation of signal transduction pathways involved in plant innate immune responses (Zhu-Salzman et al., 2004; Glazebrook, 2005). Among the signaling pathways involved in innate immune responses of plants, canonical MAPK (Mitogen-Activated Protein Kinases) signaling cascades act as bridges between diverse effectors or signal sensors and downstream defense genes (Ausubel, 2005; Pitzschke et al., 2009).

In the ongoing battlefield between plants and pathogens, the innate immunity of plants is induced by the conserved microbial feature 'microbe- or pathogen-associated molecular patterns' (MAMPs or PAMPs) and special 'effectors', which are recognized by the plant's LRR-receptor kinase, then initiate 'PAMP-triggered immunity' (PTI) and 'effector-triggered immunity' (ETI), respectively (Jones and Dangl, 2006; Chisholm et al., 2006). This host-pathogen defense model, which describes the direct or indirect recognition of pathogen Avr effectors and receptor proteins, has been genetically characterized as 'gene-for-gene' resistance (Flor, 1971). A number of resistance (*R*) genes and their direct or indirect target effectors have been cloned from many plant species and pathogens; their interaction mechanisms have also been elucidated in some cases (Chisholm et al., 2006). However, only two insect *R* genes have been cloned to date, *Mi-1* and *Bph14*, which provide resistance to the root-knot nematode (*Meloidogyne incognita*) and the brown planthopper (BPH, *Nilaparvata lugens*), respectively. Furthermore, the mechanisms whereby plants recognize the nematode or brown planthopper Avr effectors remain unknown (Rossi et al., 1998; Du et al., 2009), although RNA profiles of plant-herbivore interactions indicate that the signal perception and

transduction pathways involved may be similar to those of plant-pathogen interactions (Voelckel and Baldwin, 2004; Kaloshian and Walling, 2005; Wang et al., 2008).

Plant-herbivore interactions generally induce complex responses in plants, including the following. Various house-keeping genes that are involved in photosynthesis and general metabolism are suppressed, in plant interactions with pathogens as well as herbivores (Scheideler et al., 2002; Kaloshian and Walling, 2005). This implies that plants possess mechanisms that improve their defenses against external stress by 'sacrificing' some of the C- and N-resources required for growth and development. In addition, several important signaling pathways are activated, including JA-, Et-, and/or SA-signaling pathways following the production of reactive oxygen species (ROS). For example, JA contents increase in response to some necrotrophic fungal pathogens and arthropod herbivores, e.g. the tissue-damaging herbivores *Manduca sexta* and *Trichoplusia ni* (Farmer et al., 2003; Howe and Jander, 2008). SA is also required for the activation of systemic acquired resistance (SAR), a hypersensitive response (HR) induced by ROS that triggers a type of programmed cell death (PCD) thought to limit the access of biotrophs to water and nutrients (Glazebrook, 2005). However, it should be noted that (unlike pathogens) herbivores can avoid barren cells that have been stripped of resources by PCD since they are mobile and can thus simply move to other parts of the plant. This suggests that co-induced signaling pathways may synergistically protect plants against herbivore attack. For instance, Et sometimes acts synergistically with JA in the regulation of both stress and developmental response, in which the transcription factor (TF) Ethylene Response Factor1 (ERF1) serves as a genetic bridge between the JA and Et signaling pathways (Lorenzo et al., 2003). Further typical responses to herbivory include the activation of calcium flux and MAPK cascades, in which the calcium ions (Ca^{2+}) act as important second messengers (Maffei et al., 2007; Howe and Jander, 2008). Finally, the signaling pathways, calcium fluxes and MAPK cascades collectively activate a series of downstream defense-related genes and the production of various important protein and secondary metabolites, including pathogen-related (PR) proteins, proteinase inhibitors, polyphenol oxidases and compounds that target physiological processes in the attacking insect (Ussuf et al., 2001; Baldwin et al., 2002; Chen et al., 2005; Howe and Jander, 2008). Resistance mechanisms to phloem-feeding insects also include the induction of

forisome dispersion, callose deposition and (thus) phloem plugging, which prevent insects from continuously ingesting phloem sap from plants (Will et al., 2007; Hao et al., 2008).

MAPK cascades comprise a group of evolutionarily conserved serine/threonine-specific protein kinases in eukaryotic organisms. These protein kinases can transduce extracellular stimuli into intracellular responses by either phosphorylating a target protein in the cytoplasm or directly translocating into the nucleus and regulating gene expression through phosphorylation of specific transcription factors. These kinase cascade-mediated defense mechanisms are important signaling modules that are involved in the regulation of numerous abiotic and biotic stress responses (Jonak et al., 2002; Hamel et al., 2006; Howe and Jander, 2008). Recognition of PAMPs by plants may result in the activation of PTI via a MAPK cascade, but some bacterial effectors can block MAPK cascade-mediated innate immunity by suppressing the cascade upstream of MAPKKK (Asai et al., 2002; He et al., 2006). CTR1, a pivotal regulator involved in the ethylene signaling transduction pathway, is actually a Raf-like MAPKKK and its regulation of downstream targets is mediated by a MAPK cascade (Kendrick and Chang, 2008). Furthermore, the *AtMKK3-AtMPK6* cascade plays an important role in JA-signaling in *Arabidopsis* (Takahashi et al., 2007). Although no complete MAPK signaling pathway that provides insect resistance has been described, there is also evidence that MAPK cascades play important roles in plant-insect interactions (Kandoth et al., 2007; Wu et al., 2007). The cited studies indicate that the signaling events initiated by a diverse range of stresses have converged into a conserved MAPK cascade.

Phloem-feeding insects have a highly specialized feeding mode and cause complex damage to plants. Not only do these pests feed directly on the amino acids and carbohydrates of the host with a “stealthy” feeding mechanism, but they may also act as vectors for plant viruses or pathogens, and they may deposit honeydew, thereby encouraging the growth of mold (Brown and Czosnek, 2002; Kempema et al., 2007). The brown planthopper (BPH) is a typical phloem-feeding insect that is a significant pest of rice (*Oryza sativa* L.), causing considerable crop losses globally, especially in Asia. However, little is known about how rice perceives and resists the BPH through its innate immune system, and few genes have been reported with roles in plant defenses against

BPH infestation. An exception is *Bphi008a* (AY256682), a gene induced by both BPH-feeding and ethephon (Yuan et al., 2004). The aim of this study was to explore the defense mechanism of rice against the BPH, in particular to clarify the roles of the *Bphi008a* gene in the rice innate immunity system and resistance to the BPH.

RESULTS

Overexpression and RNAi of *Bphi008a* Affect Rice Resistance to the BPH

To clarify the role of *Bphi008a* in rice responses to the BPH, it was overexpressed (OE) or suppressed by double-stranded RNA interference (RNAi) in rice cv. Hejiang 19. Northern blot analysis showed that its expression was enhanced in six OE lines, compared with WT plants (Hejiang 19), when they were not exposed to the BPH (Figure 1A). From the T1 progeny of OE lines, we selected a homozygous transgenic plant, designated OE21-15, to generate offspring for further analyses; all of these offsprings had a single-copy insertion, according to southern blotting analysis (Figure 1C). Since the endogenous expression level of *Bphi008a* in WT plants was relatively low under normal growth conditions, the effectiveness of RNAi in six T0 transgenic lines was examined in plants that had been infested with the BPH for 48 h. The results showed that *Bphi008a* expression was blocked in RNAi plants (Figure 1B). None of the OE lines or RNAi lines exhibited obvious morphological changes (data not shown).

Fifteen-day old seedlings of the OE, RNAi and WT lines were infested with 2nd to 3rd-instar BPH nymphs at a level of seven insects per seedling. After the BPH had been feeding for 72, 96 and 120 h, all plants of each WT and transgenic line were assigned a severity score of 0, 1, 3, 5, 7 or 9 (Huang et al., 2001), and the average scores (4.2 and 7, respectively, at 96 h) clearly indicated that the OE plants had greater resistance to the BPH than WT plants (Figure 1D). In contrast, the change in susceptibility of rice to the BPH caused by RNAi of *Bphi008a* was not obvious, but we hypothesized that this may be because variety Hejiang 19 has a high susceptibility to the BPH (with a severity score exceeding 8.0). Hence it may be difficult to differentiate subtle differences in susceptibility between the WT and RNAi lines. Therefore, to evaluate further the differences in susceptibility among the WT, OE and RNAi plants, we used a real-time Electronic Penetration Graph (EPG) technique to monitor the feeding behavior of the

BPH on them (Tjallingii, 2006; Hao et al., 2008). The results showed that the duration of phloem-ingestion was approximately 40% lower on the two OE lines and approximately 15% higher on the two RNAi lines, compared with the WT plants (Figure 1E). These findings strongly indicate that the level of *Bphi008a* expression affects BPH feeding on the phloem of rice. Finally, the honeydew area was measured after the BPH had been feeding for 48 and 72 h. Clear differences were observed between the OE and WT plants (Figure 1F), supporting the suggestion that *Bphi008a* expression enhances rice resistance to the BPH by impairing BPH feeding.

Selection of House-keeping Genes for Real-time PCR during BPH-feeding on Rice

As mentioned in the Introduction, some house-keeping (HK) genes are suppressed in host-herbivore interactions. The current consensus is that multiple stably expressed HK genes are required for accurate and robust normalization (Schmittgen and Zakrajsek, 2000; Vandesompele et al., 2002). Therefore, to characterize changes in gene expression following BPH feeding on the wild type (WT) and transgenic lines as accurately as possible by real-time PCR, we chose the most stably expressed candidates for normalization from the following 10 commonly used rice HK genes: *β-actin*, *LSD1*, *GAPDH*, *eEF1α*, *SDHA*, *TBP*, *RPS27α*, *HSP*, *β-tubulin* and *ubiquitin*. These genes all belong to different functional classes, reducing the chances of co-regulation (detailed information on the HK genes is provided in Supplemental Tables 1 and 2). The comparative expression levels of each HK gene, at seven time-points (0, 6, 12, 24, 48, 72 and 96 h after the BPH had been feeding on leaf-sheaths), were determined by real-time PCR.

Using the geNorm algorithm, we ranked these 10 HK genes according to their comparative expression stability at the seven time-points (Vandesompele et al., 2002). As shown in Figure 2, the results indicated that the most stably expressed combinations of HK genes were: *β-tubulin*, *HSP* and *ubiquitin* (in WT plants alone); *TBP*, *ubiquitin* and *HSP* (in OE and WT plants); *TBP*, *ubiquitin* and *β-tubulin* (in RNAi and WT plants); and *LSD1* and *ubiquitin* (in WT controls and WT plants pretreated with the ethylene competitive inhibitor 1-MCP). To confirm the results of the geNorm algorithm, we also used another algorithm, NormFinder (Andersen et al., 2004), to examine qPCR data of these 10 HK genes. This gave almost identical ranking trends for the genes to those of the

geNorm algorithm, except for some minor differences that we attributed to the different emphases of the algorithms (Supplemental Figure 1). After we had identified the most stably expressed HK genes in the studied lines, we used the Biogazelle qBasePlus relative quantification framework for further analysis of the real-time PCR data (Hellemans et al., 2007).

Bphi008a Is a Downstream Gene of the Ethylene Signaling Pathway in Rice

In a previous study, *Bphi008a* expression was found to be induced by both BPH feeding and spraying plants with ethephon, which slowly releases ethylene (Yuan et al., 2004). Therefore, we investigated changes in the expression of genes involved in ethylene biosynthesis in rice plants that had been fed upon by the BPH. In rice, a large gene family controls ethylene biosynthesis, composed of six ACC synthase genes (designated *OsACS1* to *OsACS6*) and seven ACC oxidase genes (designated *OsACO1* to *OsACO7*) (Yang and Hoffman, 1984; Iwai et al., 2006). We found that expression levels of all of the ethylene biosynthesis genes were increased after BPH-feeding, except *OsACS1*, *OsACS3* and *OsACO4*, whose transcription was not detected in rice cv. Hejiang 19 (data not shown). Expression levels of three members of the ACC synthase subfamily (*OsACS2*, *OsACS4* and *OsACS5*) were increased after BPH-feeding for 6 h, then *OsACS2* and *OsACS5* expression levels remained high until 96 h, while *OsACS4* expression levels were increased two-fold after 6 h, but then decreased to control levels. *OsACS6* expression levels were almost unaffected by BPH-feeding before 48 h, but then began to decrease (Figure 3A). In addition, expression levels of four members of the ACC oxidase subfamily (*OsACO1*, *OsACO2*, *OsACO3* and *OsACO7*) had all increased by 6 h, but then began to decrease and reached their lowest levels after 96 h of BPH feeding. *OsACO5* expression levels were increased until 24 h of BPH feeding, but then subsequently declined to just a quarter of control levels after 96 h (Figure 3B). Further, as shown in Figure 3C, ethylene measurements at 3, 6, 12, 24, 48 and 72 h time points showed that levels of ethylene emitted from WT plants rapidly increased upon BPH-feeding, and were maximal at the end of the monitoring period (72 h). These results suggest that BPH feeding rapidly initiated ethylene biosynthesis.

In addition, we used 1-methylcyclopropene (1-MCP; C_4H_6), a volatile gas and ethylene inhibitor that competitively binds to the ethylene receptor in plants, to block transduction

of ethylene signals. We pretreated WT plants for 48 h with 1-MCP (10 ppm), then investigated changes in the expression levels of *Bphi008a* after 0, 6, 12, 24, 48, 72 and 96 h of BPH-feeding in these and control plants (which received no 1-MCP treatment). *Bphi008a* expression levels increased from 0 h to 96 h in the controls, but in Hejiang 19 plants pretreated with 1-MCP, *Bphi008a* expression levels were very low (Figure 3D). We also found no significant differences in the expression levels of *OsACO*s and *OsACS*s between the WT and transgenic plants, except that *OsACO1* expression was increased after BPH-feeding for 96 h and *OsACO2* after BPH-feeding for 72 and 96 h in the OE plants (Supplemental Figure 2). Together, these results indicate that *Bphi008a* transcription is stimulated by active ethylene and *Bphi008*a is a downstream gene of the ethylene signaling pathway in rice.

Detection of *Bphi008a* Expression Patterns and Localization in Rice

We examined relative expression levels of *Bphi008a* in leaf-sheaths, stems, leaf-blades and roots of seedlings, and leaf-sheaths, leaf-blades and flowers of plants at the heading stage. Using the NormFinder algorithm, we chose *LSD1* as the most stably expressed HK gene in these seven types of samples (Supplemental Figure 3). We found that *Bphi008a* expression levels were highest in the roots of seedlings, followed (in order) by leaf-blades and leaf-sheaths at the heading stage, then leaf-sheaths, leaf-blades and stems of seedlings. The lowest detected level of *Bphi008a* expression was in the flowers (Figure 4).

SMART sequence analysis by the Bork Group (http://www.bork.embl.de/j/) has shown that Bphi008a has an N-terminal transmembrane region, somewhere between amino acid positions 7 and 29. To obtain preliminary indications of the function of *Bphi008a*, we determined its subcellular localization by translationally fusing full-length Bphi008a to the C-terminal of the yellow fluorescent protein, and expressing the chimeric protein under the control of the CaMV35S promoter. In addition, we truncated the gene by removing the sequence encoding the 20 N-terminal amino acids, which might be the main transmembrane region of Bphi008a, and cloned the rest of the coding sequence (designated *tnBph8a*) into the C-terminal of the yellow fluorescent protein. Onion (*Allium cepa*) epidermal cells transiently expressing the YFP without Bphi008a showed signals throughout cells (Figure 5A). We found that the YFP-tnBph8a fusion protein lost its

plasma membrane localization and was mainly localized in the cytosol, or in both the cytosol and nucleus (Figures 5B and 5C), while cells transiently expressing the YFP-Bphi008a fusion protein predominantly showed YFP signals at the plasma membrane and nucleus (Figure 5D). These results suggest that *Bphi008a* has dual localization and its N-terminal amino acids are likely to be involved in its localization.

Bphi008a Is Phosphorylated by OsMPK5 *in Vitro*

In attempts to elucidate the function of Bphi008a in signal transduction processes, we first analyzed its possible motifs. In the C-terminal proline-rich region of Bphi008a, we found several proline-related motifs, including two Pro-X-X-Pro motifs and one Pro-Pro-Gly-Arg motif (Figure 6A; Kay et al., 2000; Kofler and Freund, 2006). In addition, two robust, comprehensive motif search algorithms, Scansite 2.0 and Eukaryotic Linear Motif (ELM), showed that it has a putative MAPK phosphorylation site and a conserved docking site for a proline-directed MAPK at positions between amino acids 52 and 58 (Obenauer et al., 2003; Puntervoll et al., 2003). These findings suggested that it might be post-translationally regulated through phosphorylation. *OsMPK5*, which is also involved in disease resistance and abiotic stress tolerance, was identified as a candidate target kinase for Bphi008a (Xiong and Yang, 2003). In addition, we cleaved the C-terminal 29 amino acids of Bphi008a to use the remaining coding sequence (designated *tBph8a*) as a negative control (Figure 6A). We produced glutathione S-transferase (GST) fusion proteins containing OsMPK5, Bphi008a and tBph8a in *Escherichia coli*, and purified them. We then assayed their kinase activity *in vitro*, after checking the amounts of GST, GST-MPK5, GST-Bphi008a and GST-tBph8a proteins by 12% (w/v) SDA-PAGE analysis (Figure 6B). The results showed that GST-MPK5 has concentration-dependent autophosphorylation ability and the capacity to phosphorylate GST-Bphi008a. When less than 4 μg GST-MPK5 was used in the assays, it showed strong autophosphorylation ability and we only detected weak GST-Bphi008a phosphorylation (Figure 6C, Lanes 1-4). However, when we increased the amounts of GST-MPK5 to 16 μg, we detected a strong GST-Bphi008a phosphorylation band, accompanied by abatement of GST-MPK5 autophosphorylation (Figure 6C, Lane 6). Furthermore, no phosphorylation interaction between GST-MPK5 and GST-tBph8a was detected (Figure 6C, Lane 8). These results indicate that phosphorylation of Bphi008a's

C-terminus motif might have a function *in vivo*.

Bphi008a Interacts with OsMPK5 in the Nucleus

Since the interaction between OsMPK5 and Bphi008a involved phosphorylation *in vitro*, we wanted to determine whether or not these two proteins could interact *in vivo*. For this purpose, complete *Bphi008a*, *tBph8a* and *OsMPK5* coding sequences were separately cloned into pGADT7 and pGBKT7 vectors to create a yeast two-hybrid system. Among all 17 mating combinations, we found one (designated No. 15) in addition to the positive control that showed a clear positive interaction on the QDO/X-α-Gal plate, which corresponded to 'pGBKT7-OsMPK5' mating with 'pGADT7-Bphi008a' (Supplemental Table 3 and Figure 6D). In addition, Nos. 12 and 16 (corresponding to 'pGBKT7-Bphi008a' mating with 'pGADT7- OsMPK5' and 'pGBKT7-OsMPK5' mating with 'pGADT7-OsMPK5', respectively) showed comparatively weak interactions. These findings imply that OsMPK5 has weak ability to interact with itself *in vivo*, in contrast to the strong autophosphorylation capacity observed *in vitro* (Figures 6C and 6D). Relative β-galactosidase activities were also measured, and provided results consistent with those from the QDO/X-α-Gal/3-AT plate (Figure 6E).

Following the confirmation that Bphi008a can interact with OsMPK5 in yeast cells, we tested the possibility that these two proteins interact in plant cells, using a particle gun–mediated system. We found that OsMPK5 also had dual localization, coinciding with that of Bphi008a (Figure 5E), and postulated that if these two proteins interact in plant cells, they presumably do so in the nucleus and/or the plasma membrane. To test this hypothesis, we transiently coexpressed Bphi008a (or tBph8a) tagged with pSPYNE (split YFP N-terminal fragment expression) and OsMPK5 tagged with pSPYCE (split YFP C-terminal fragment expression) using *Arabidopsis* protoplast transfection (Walter et al., 2004; Yoo et al., 2007). As anticipated, the results indicated that Bphi008a and OsMPK5 can interact with each other in the nucleus, but not in the plasma membrane. Meanwhile, we detected no interaction between tBph8a and OsMPK5 in protoplasts (Figure 6F). Similar bimolecular fluorescence complementation (BiFC) results were observed in onion epidermal cells using the particle gun–mediated system (Supplemental Figure 5).

Bphi008a Overexpression and RNAi Result in Different *OsMPK*s Expression Patterns

The BiFC and kinase assay results showed that OsMPK5 can interact with Bphi008a by mediating its C-terminal proline-directed phosphorylation, and that this interaction occurs in the nucleus. We speculated that phosphorylated Bphi008a plays a role in *MAPK* signaling pathways. In rice, we had identified 17 members of the *MAPK* family (*OsMPK1* to *OsMPK17*), four of which (*OsMPK5*, *OsMPK12*, *OsMPK13*, *OsMPK17*) can be induced by both treatment with 1-aminocyclopropane-1-carboxylic acid (ACC, an ethylene precursor) and pathogen (*Magnaporthe grisea*) infection (Reyna and Yang, 2006). We found that expression levels of these four genes also increased in response to BPH-feeding (most strongly after 96 h, except for *OsMPK17*, which was only induced after the BPH had been feeding for 6 h; Figures 7A to 7D). These findings suggested that the conserved *MAPK* signaling pathways serve as bridges in responses to hormones and biotic stresses. In the OE plants (OE21-15), we found that expression levels of these four genes increased compared with WT, in both controls and plants fed on by the BPH (Figures 7A to 7D). However, we found that expression levels of both *OsMPK12* and *OsMPK17* remained unchanged in *Bphi008a*-suppressed (RNAi7) plants that had not been exposed to the BPH, but they declined after BPH-feeding, compared with levels in WT and OE plants (Figures 7B and 7D). Furthermore, *OsMPK5* expression levels increased before the BPH had been feeding for 24 h, compared with levels in WT plants, but decreased notably in response to BPH-feeding from 24 to 96 h in RNAi plants (Figure 7A). Unexpectedly, *OsMPK13* expression levels were increased in both OE and RNAi plants, compared with WT plants (Figure 7C). In addition, immunoblot analysis showed that the OsMPK5 protein level was increased after BPH had been feeding for 6 h and remained at a high level until 96 h in the WT plants. Compared with the WT plants, OE plants had consistently higher OsMPK5 protein levels, and RNAi plants significantly lower levels, after BPH-feeding (Figures 8A and 8B). These results suggest that *Bphi008a*- induced resistance to BPH is directly related to the *MAPK* signaling pathway and one or more other genes may mediate the regulation of *MAPK* expression after BPH-feeding. This could partly compensate for the reduction in *Bphi008a* expression caused by RNAi, such as *OsMPK13*. The expression levels of the *OsMPK*s increased in

OE lines following BPH feeding, therefore some downstream transcription factors and defense-related genes might be activated, finally resulting in increased resistance to the BPH.

Bphi008a Overexpression Enhances Levels of AP2/ERF Transcription Factors and Defense-related Genes

Recently there have been claims that ethylene inactivates the negative regulator CTR1 in *Arabidopsis*, thereby activating a positive AtMKK9-AtMPK3/6 cascade that targets EIN3 through two MAPK phosphorylation sites (Yoo et al., 2008). Transcription factor EIN3/EIL is a key component of the primary ethylene signaling pathway and the AP2/ERF transcription factor ERF1 serves as an immediate target for EIN3 in *Arabidopsis* (Guo and Ecker, 2004). Overexpression of *ERF1* in *Arabidopsis* is sufficient to confer resistance to several necrotrophic fungi, such as *Botrytis cinerea* and *Plectosphaerella cucumerina* (Berrocal-Lobo et al., 2002). These findings have established that a linear AtMPK3/6-AtEIN3-AtERF1 signaling pathway in the nucleus participates in responses to external biotic stresses. The rice gene *OsMPK5* has high similarity to *AtMPK3* and both are associated with diverse biotic and abiotic stress responses (Mizoguchi et al., 1996; Xiong and Yang, 2003). In addition, *OsMPK12*, originally named *OsBWMK1*, mediates expression of pathogen-related genes by phosphorylation-mediated activation of an AP2/ERF transcription factor, *OsEREBP1*, and enhances resistance of tobacco to the virulent oomycete pathogen *Phytophthora parasitica* var *nicotianae* (Cheong et al., 2003). This evidence suggests that a linear OsMPK5/12-OsERF1/OsEREBP1 signaling pathway may mediate responses to external biotic stresses in rice. We found that expression levels of *OsERF1* and *OsEREBP1* were also enhanced in OE plants, compared with WT plants (Figures 8C and 8D), suggesting that *Bphi008a*-mediated enhancement of plant resistance to the BPH might be correlated with the activation of defense-related genes by some specific transcription factors.

We hypothesized that the suppression of BPH-feeding in the *Bphi008a* OE lines described above (Figures 1E and 1F) may be ultimately related to the upregulation of some defense-related genes, which could thwart BPH-feeding. Some well-studied JA-inducible proteinase inhibitors (PIs) in tomato plants are reportedly involved in plant resistance to herbivorous insects by disrupting digestive processes in their gut. These PIs

include arginase, threonine deaminase (TD), cysteine protease inhibitor (CysPI) and leucine aminopeptidase A (LEA). Arginase catabolizes the essential amino acid Arg in the *M. sexta* midgut, and thus interferes with digestive processes, thereby increasing the resistance of tomato to *M. sexta* larvae (Chen et al., 2005). Our analyses showed that *Arginase* expression levels were increased in OE plants and somewhat decreased generally in RNAi plants when fed on by the BPH (Figure 8E). Furthermore, we found that the expression levels of (especially) *LEA2* and *CysPI* were also enhanced in the OE plants (Figures 8F and 8G). These results may explain why BPH feeding behavior was suppressed in OE plants.

Bphi008a Interacts with OsbZIP60 and SDRP in Yeast Cells

Bphi008a is clearly not an upstream gene of *MAPK* signaling pathways, so we speculated that the function of phosphorylated Bphi008a could be related to transcriptional regulation. Since Bphi008a has no DNA-binding domain, unlike many traditional transcriptional factors, we surmised that it may be a key member of a transcriptional complex, and thus could regulate the transcription of *OsMPK*s, via interactions between the Pro-X-X-Pro or Pro-Pro-Gly-Arg motifs and other components of the transcription machinery. To test our conjecture, Bphi008a was used as a bait to screen a prey cDNA rice library. The yeast two-hybrid screening resulted in 20 unique genes encoding putative Bphi008a-interacting proteins (BIPs). The predicted functions of BIPs are quite diverse, but can be classified into five categories (Figure 9A and Supplemental Table 4). Among them, we found two clones (Os03g0102200 and Os06g0622700) related to transcription regulation. Os03g0102200 is a 14.5 kDa polypeptide that is similar to DNA-directed RNA polymerase II, and we renamed it SDRP, while Os06g0622700 is a bZIP (basic leucine zipper) transcription factor that shows the highest homology to AtbZIP60 in *Arabidopsis* (Supplemental Figure 6), so we renamed it OsbZIP60.

Complete *Bphi008a* and *OsbZIP60* (or *SDRP*) coding sequences were cloned into pGBKT7 and pGADT7 vectors, respectively, to create a yeast two-hybrid system. As shown in Figure 9B, we detected a clear interaction between Bphi008a and OsbZIP60. In addition, we detected a weak interaction between Bphi008a and SDRP. Furthermore, analysis of *OsbZIP60* expression levels in WT and transgenic plants after BPH-feeding

from 0 h to 96 h (Figure 9C) indicated that Bphi008a (possibly phosphorylated) might form a transcriptional complex with OsbZIP60 and SDRP *in vivo* that activates the transcription of target genes.

DISCUSSION

Rice-BPH Interactions Are Complicated and Might Involve Multi-signaling Pathways

What signaling pathway(s) activated caused by extracellular stress is (are) essential for plants to turn on the appropriate defense pathways in their innate immune systems. Our results indicate that when the BPH feeds on rice, upstream genes involved in ethylene production are rapidly upregulated, within 6 h, and ethylene emission is continuously enhanced thereafter until 72 h (Figures 3A, 3B and 3C). In addition, transcript levels of two JA synthesis-related genes, *AOS2* (encoding allene oxide synthase 2) and *DoX2*, and two SA synthesis-related genes, *PAD4* (phytoalexin deficient 4) and *PAL* (encoding phenylalanine ammonia-lyase) are continuously enhanced for at least 96 h during BPH-feeding (Zhou et al., 1998; Glazebrook, 2005; Wei et al., 2009; Supplemental Figure 7A). ERF1 is a member of the AP2/ERF transcription factor and plays a key role in the integration of JA and Et signals, thereby activating Et/JA-dependent responses to pathogens (Lorenzo et al., 2003). Our findings show that the expression of *OsERF1* increases after BPH-feeding, implying that a combined Et/JA signaling pathway might be involved in the defense of rice against the BPH (Figure 8B). Thus, these results collectively indicate that BPH-feeding not only induces the Et signaling pathway, but might also activate JA and SA signaling pathways. However, as the BPH-feeding time increased, especially after the BPH had been feeding for 24 h, we found that expression levels of all *OsACO* genes and *OsACS4* began gradually to decrease, and all were lowest at the end of the monitoring period (96 h), compared with WT levels (Figures 3A and 3B). These changes in relative expression levels are very different from the pattern displayed by genes encoding components of the SA/JA pathways, whose expression levels consistently increased during BPH feeding (Supplemental Figure 7A). These findings suggest that the BPH can protect itself from defenses induced by the Et signaling pathway by preventing the expression of some genes that participate in this pathway, in latter stages of its feeding. Several researchers have reported analogous findings. For

example, caterpillar (*Helicoverpa zea*) and silverleaf whitefly (*Bemisia tabaci* type B; SLWF) can suppress JA defenses by inducing SA defenses (Musser et al., 2002; Zarate et al., 2007). These results suggest that the BPH might introduce effector proteins to plant cells that suppress certain signaling pathways and thus protect itself, in a similar fashion to the suppression of PTI by microbial pathogens (Chisholm et al., 2006; Jones and Dangl, 2006). Moreover, we also observed increased expression of many downstream pathogen-related (PR) genes, which was maximal at the end of the monitoring period, after 96 h of BPH feeding (Supplemental Figures 7B and 7C). In conclusion, when the BPH feeds on rice, it can immediately activate the Et signaling pathway; Rice-BPH interactions are complicated and might involve JA and SA signaling pathways.

*OsMPK*s Are Involved in Immune Responses of Rice to the BPH

The way in which signals are transducted is key in the activation of the correct downstream targets of defense pathways in plants. Phosphorylation is an important post-translational modification and a major regulatory mechanism that is estimated to affect a third of the proteome and that controls many cellular signaling pathways (Ptacek et al., 2005). Conserved MAPK cascades play a key role (through series of phosphorylations) in the establishment of resistance to external stimuli in all eukaryotes (Ausubel, 2005). On the basis of experiments using transient expression in *Arabidopsis* protoplasts, the MAPK cascade MEKK1-MKK4/MKK5-MPK3/MPK6-WRKY29, in which WRKY29 could bind to W-box DNA elements (TGAC core sequence) that found in the promoters of many defense-related genes, has been proposed to be responsible for flg22-induced defense response (Asai et al., 2002). Seventeen *MAPK* genes have been identified in the rice genome, yet little is known about how these *OsMPK*s are involved in defense responses to herbivore attack through the innate immune system in rice. In our research, the expression levels of four *MAPK* genes (*OsMPK5*/*12*/*13*/*17*), which were also induced by ACC and *M.grisea*, were enhanced in response to BPH-feeding (Figure 7). In addition, the protein levels of OsMPK5 were also increased in WT and OE plants exposed to BPH-feeding (Figures 8A and 8B). Although *OsMPK1/5* has a high similarity to *AtMPK6/3*, we found that *OsMPK1* does not respond to introduction of the pathogen *M.grisea* or to BPH-feeding (Reyna and Yang, 2006; unpublished data). These findings suggest that regulation patterns in response to biotic stresses differ between *Arabidopsis*

and rice. Furthermore, *OsMPK5/12* can activate some downstream transcription factors, such as *OsERF1* and *OsEREBP1*, through phosphorylation, which enhances their ability to bind to the target sequence AGCCGCC (i.e. the GCC box) contained in some defense-related gene promoters and further activate their transcription (Figures 8C and 8D; Cheong et al., 2003; Gutterson and Reuber, 2004). In the present study, we found that OsMPK5 could also phosphorylate Bphi008a *in vivo*. Finally, we found enhanced expression levels of some downstream defense-related genes, such as *Arginase*, *LEA2* and *CysPI*, which can hinder digestive processes in the insect midgut (Figures 8E, 8F and 8G). Since it is unclear whether there is a direct relationship between OsERF1/OsEREBP1 or Bphi008a and the activation of *Arginase*, *CysPI* or *LEA2*, this warrants further investigation. However, our results demonstrate that several *OsMPK* genes play an important role in response of rice to the BPH.

Bphi008a Might be Involved in Stress Response through Interaction with OsbZIP60

The yeast two-hybrid screening results showed that Bphi008a can interact with transcription factor OsbZIP60, a homolog of AtbZIP60 in *Arabidopsis thaliana* and NtbZIP60 in *Nicotiana tabacum* (Supplemental Figure 6). The membrane-bound transcription factor AtbZIP60, the activity of which is controlled by proteolytic cleavage, is considered to function as a sensor for Endoplasmic Reticulum (ER) stress and may regulate the expression of many ER chaperone genes by activating plant-UPR and ERSE *cis*-elements (Iwata et al., 2005; Iwata et al., 2008). Furthermore, size exclusion chromatography analysis has shown that the nuclear form of AtbZIP60 exists as a protein complex of approximately 260 kDa (Iwata et al., 2009). There has been limited research on the link between biotic stress defense and stress response in plants, but NtbZIP60 is reportedly involved in defense responses to the non-host pathogen *Pseudomonas cichorii* and plays an important role in plant innate immunity (Tateda et al., 2008). Our result demonstrates that BPH-feeding could suppress *OsbZIP60* expression levels before 72 h, this is a different outcome from that of treatment with tunicamycin in *Arabidopsis* or inoculation with the non-host pathogen *Pseudomonas cichori* in *Nicotiana* (Figure 9C; Iwata et al., 2008; Tateda et al., 2008). These differences hint that the BPH may protect itself by introducing effector proteins that suppress stress responses. In the OE and RNAi plants, we also detected the upregulation and downregulation of *OsbZIP60*, respectively

(Figure 9C). We suggest that Bphi008a might involve in the transcription of some *OsMPK*s through combination with OsbZIP60 and SDRP (Figure 9B). Interestingly we found that the expression levels of *OsMPK13* and *CysPI* were also enhanced in RNAi plants (Figures 7C and 8F). We hypothesize that other genes, besides *Bphi008a*, may also mediate defense responses of rice to the BPH through MAPK cascades, which could compensate for the RNAi-induced reduction of *Bphi008a* expression. Isolation and characterization of proteins that interact with the nuclear form of OsbZIP60 and examination of the mechanism whereby the phosphorylated (or non-phosphorylated) form of Bphi008a binds to OsbZIP60 in plant cells should yield valuable insights in this context. In addition, we should unravel how the OsbZIP60 transcription complex activates *cis*-elements of *OsMPK*s through Chromatin Immuno-Precipitation (ChIP) analysis. Research in this area is currently underway.

MATERIALS AND METHODS

Gene Constructs and Rice Transformation

To make an overexpression construct, the *Bphi008a* coding sequence was cloned into the plasmid vector pAHC17. The resulting recombinant *pAHC17-Bphi008a* vector was sequenced to ensure the correct insert. After digestion of the *pAHC17-Bphi008a* vector with EcoRI and HindIII, the insert was ligated in frame into the plasmid vector pCAMBIA1301 to make the overexpression construct (*Bphi008a-OE*).

To make a dsRNAi construct, the complete *Bphi008a* sequence was cloned into the XhoI-EcoRI restriction enzyme sites in the pHANNIBAL vector (Wesley et al., 2001), thus creating *pHAN-Bph8a1*. The PCR fragment generated using the XbaI-HindIII pair of primers (to form the antisense fragment) was also XbaI-HindIII digested and cloned into the same sites in *pHAN-Bph8a1* to create *pHAN-Bph8a2*. The *pHAN-Bph8a2* vector was digested with *NotI* and the insert was ligated in frame into the plasmid vector pART27 to form the dsRNAi construct (*Bphi008a-RI*). Overexpression and dsRNAi constructs were introduced into *Agrobacterium tumefaciens* (strain LBA4404) by electroporation, using vigorously growing calli derived from mature embryos of rice cv. Hejiang 19 following standard procedures (Hiei et al., 1994). T0 transgenic plants were grown in a greenhouse under 14 h light/10 h dark cycles at 28°C.

Plants, Insects and BPH-resistance Evaluation

Japonica rice (*Oryza sativa*) variety Hejiang 19, a line that is susceptible to the BPH with a severity score exceeding 8.0 in seedling bulk tests, was used in this study. Unless otherwise stated, the brown planthopper (*Nilaparvata lugens* Stål; BPH) insects were maintained on TN1 plants in the Genetics Institute, Wuhan University, and 2nd to 3rd instar nymphs were used in experiments (all of which were carried out on rice plants at the three-leaf stage).

EPG recordings were carried out for 8 h/insect/plant, with at least five replicates for each variety (using fresh seedlings and insects in each case), and the data acquired were analyzed as previously described (Hao et al., 2008). Honeydew area evaluation was carried out for 48 and 72 h/four insects/plant, with eight replicates for each variety. After the experiment was finished, the filter papers were rinsed with 0.25% ninhydrin and color-developed in a 55°C drying oven. Photoshop 7.0 was used to calculate the percentage of colored area to total area.

DNA Isolation and Southern-blot Analysis

Genomic DNA was extracted from rice leaves of WT (cv. Hejiang 19) and transgenic plants using the CTAB (cetyltrimethyl ammonium bromide) method. The genomic DNA was digested with the restriction endonuclease DraI, then electrophoretically separated on a 0.8% agarose gel, transferred onto a Hybond N^+ membrane (Amersham-Pharmacia, USA), then probed with *Bphi008a* cDNA labeled with [α-^{32}P] dCTP using the Prime-a-Gene labeling system (Promega, USA). The blots were hybridized for more than 10 h at 65°C with the labeled probe, washed at 65°C for 15 min in 1x SSC and 0.2% SDS, then kept at 65°C for 15 min in 0.5x SSC and 0.1% SDS. The membranes were finally exposed to X-ray film for autoradiography.

RNA Isolation, Northern-blot Analysis and First-strand cDNA Synthesis from RNA

Total RNA was extracted from 15-day-old seedling tissue frozen in liquid nitrogen using TRIzol reagent (Invitrogen, USA) followed by isopropyl alcohol precipitation. The RNA was then dissolved in DEPC-treated water. The concentration of RNA was determined by spectrophotometric measurements (Perkin-Elmer, USA). For northern blot analysis, total RNA (10 μg) was separated on a 1.5% formaldehyde agarose denaturing

gel, then blotted onto Hybond N^+ nylon membranes. Full-length *Bphi008a* cDNA probes were labeled with [α-^{32}P] dCTP. Hybridization was performed for more than 10 h at 55°C, then membranes were washed with 1x SSC and 0.2% SDS at 55°C for 15 min, followed by 0.5 x SSC and 0.1% SDS at 55°C for 15 min. The membranes were finally exposed to X-ray film for autoradiography.

cDNA was synthesized using the oligo$(dT)_{18}$ primer and a RevertAid^{TM} First Strand cDNA Synthesis Kit (Fermentas) according to the manufacturer's instructions, using 3 μg total RNA from each sample for reverse transcription. The cDNA was diluted 10-fold and amplified for real-time PCR analysis.

Protein Extraction and Immunoblot Analysis

Samples (0.125 gram) of 15-day-old seedlings were ground to powder with liquid nitrogen and homogenized in 750 μL extraction buffer (0.1 M Tris-HCl PH 7.5, 5 mM $MgCl_2$, 1 mM EDTA, 0.05% Triton X-100 and 2 mM DTT). After 2 h incubation on ice, the homogenate was centrifuged for 15 min at 20,000g at 4°C, and the resulting supernatant was used for immunoblot analysis. Fifty μg (about 12 μL) of supernatant was mixed with 4 μL of 4 x SDS sample buffer (250 mM Tris-HCl pH6.8, 40% glycerol, 6% SDS, 20% β-mercaptoethanol and 0.04% Bromophenol blue) and boiled for 8 min. The samples were then analyzed by 12% (w/v) SDS–PAGE. After electrophoresis, proteins were electroblotted to nitrocellulose membranes. Membranes were blocked in 5% nonfat dried milk in TBS-T (20 mM Tris-HCl pH 7.6, 137 mM NaCl and 0.1% Tween 20) overnight at 4°C and then washed for 3 x 8min in TBS-T. The membranes were incubated with the rabbit OsMPK5 polyclonal antibody (1:1000) or with the mouse HSP82 monoclonal antibody (1:10000) diluted with 1% BSA in TBS-T for 1.5 h at room temperature. Next, the membranes were washed in TBS-T for 3 x 8min, and incubated for 1.5 h with goat anti-rabbit IgG or goat anti-mouse IgG (1:10000 dilution in TBS-T and 1% BSA) conjugated to alkaline phosphatase, followed by a further 3 x 8min in TBS-T. Finally, OsMPK5 was detected using 5-bromo-4-chloro-3-indolyl phosphate/nitroblue tetrazolium (BCIP/NBT) as the substrate.

Primer Design and Real-time PCR Analysis

The primers used for real-time PCR were designed using Beacon Designer 7.5 software according to mRNA sequences obtained from NCBI GenBank. Reactions were

carried out using a Rotorgene 6000 real-time PCR system (QiaGene) with the following temperature profile: 95°C for 2 min, followed by 34 cycles of 95°C for 5 s, 55°C for 5 s, and 72°C for 10 s. After the amplification, a melting curve was determined for each primer pair across a temperature range from 72°C to 98°C to verify that only one specific product was present. A standard curve for each gene was also determined. The reactions were performed in triplicate and the results were averaged. All of the primer data from this study can be found in Supplemental Tables 1, 2 and 5. Last, we also determined comparative expression levels of all genes normalized to the same transcripts (*TBP* and *HSP*) amongst the WT, OE and RNAi lines. The results showed almost the same comparative expression levels as those from OE, RNAi and WT lines, separately (Supplemental Figure 8; Supplemental Table 6)

Measurement of ET Emission

Twenty 15-day-old seedlings were placed in a gas-proof transparent plastic housing (diameter 15cm, height 50cm) and left in a growth cabinet at 28±2°C for 12 h under light. At 3, 6, 12, 24, 48 and 72 h after the start of BPH-feeding, 1 ml of gas was withdrawn from the airspace of each plastic housing using a gas-tight syringe (Agilent) and injected into a gas chromatograph (Agilent GC-6890N) equipped with an aluminum column (Shumpak-A; Shimazu) and a flame-ionization detector for ET determination.

1-MCP Treatment

For the 1-MCP treatment, 15-day old seedlings were transferred into a hermetic glass house (~5m^3) and sprayed with the 1-MCP at a final concentration of 10 ppm. After two days, the pretreated plants were transferred into a greenhouse under 14 h light/10 h dark cycles at 28°C for BPH-feeding.

Subcellular Localization, dapi and FM4-64 Staining

For the analysis of the subcellular localization of Bphi008a and tnBph8a, the *Bphi008a*, *tnBph8a* and *OsMPK5* coding sequences were cloned in frame to a C-terminal Bsp1407I site and XbaI site of *YFP*, respectively, using the *pBS-35S-YFP* vector. Onion epidermal cells were then bombarded with recombined constructs using a particle gun–mediated system (PDS-1000/He; Bio-Rad) and analyzed by confocal microscopy (FV10-ASW; Olympus).

For dapi staining, onion epidermis was dyed for 10 min in dapi (1 μg/ml) and then rinsed in PBS solution before being examined under the confocal microscope. For dapi and FM4-64 counterstaining, after dapi staining and rinsing, onion epidermis was re-dyed with FM4-64 (10 nM) for 10 min and examined under the confocal microscope.

Expression and Purification of Recombinant Proteins

For expression and purification of GST-MPK5, GST-Bphi008a and GST-tBph8a proteins, the coding sequences were cloned into the BamHI and XhoI site of the pGEX-6P-1 expression vector (GE Healthcare, Sweden). *E. coli* BL21 cells were transformed with the three recombinant plasmids and grown to an OD_{600} of 0.6. Expression of the recombinant proteins was then induced with 0.5 mM IPTG (isopropyl *β*-D-thiogalactopyranoside) for 5 hr at 37°C. Bacteria culture (100 ml) was centrifuged at 12000g for 10 min and the sedimented bacteria were resuspended in PBS buffer (1x PBS, 1 mM PMSF, 1 mM DTT, 0.1 mM $MgCl_2$ and 1% Triton X-100) for ultrasonication. Most of the GST-Bphi008a and GST-tBph8a fusion proteins were insoluble, being localized in inclusion bodies (data not shown). Therefore, the inclusion bodies were resuspended in lysis buffer (50 mM Tris-HCl pH 8.0, 0.1 mM EDTA, 5% glycerol, 0.1 mM DTT and 0.1 M NaCl) containing 0.3% SKL (sodium lauroylsarcosine). The proteins (GST-Bphi008a and GST-tBph8a) were then renatured in dialysis bags at 4°C for 24 h in refolding buffer (50 mM Tris-HCl pH 8.0, 0.5 mM EDTA, 5% glycerol, 0.1 mM DTT and 0.05 M NaCl). Soluble GST-MPK5, renatured GST-Bphi008a and GST-tBph8a proteins were purified by passage through High-Affinity GST Resin (GenScript Corporation, USA) and their concentrations were determined using a Bradford Protein Assay Kit (Beyotime, China).

***In Vitro* Kinase Assay**

Phosphorylation assays were performed by incubating (at 30°C for 2 h) 30 μL reaction mixtures containing 0.5-16 μg of GST-MPK5 kinase and 4 μg of GST, GST-Bphi008a or GST-tBph8a with 20 mM Tris-HCl pH 7.5, 1 mM DTT, 10 mM $MgCl_2$, 50 μM unlabeled ATP, 0.1 mM $NaVO_3$ and 5 μCi of γ-^{32}P-ATP (6000 Ci/mmol; Amersham Pharmacia Biotech). The reaction was stopped by adding 10 μL of 4x SDS sample buffer and boiling for 8 min. The samples were then analyzed by 12% (w/v) SDS–PAGE and subjected to

autoradiography.

Yeast Two-hybrid Assay and Screening

The Matchmaker™ gold yeast two-hybrid system (Clonetech) was used to confirm the interactions between Bphi008a (or tBph8a) and OsMPK5, and the interaction between Bphi008a and OsbZIP60 (or SDRP). Complete *Bphi008a* and *tBph8a* coding sequences were separately cloned in frame to the EcoRI and BamHI site of the pGADT7 and pGBKT7 vectors, respectively. The complete *OsMPK5* (AF479883) coding sequence was amplified from mRNA by nested-PCR using the first round primers 5'-ATTAGGTTG GTCAATTCG-3' with 5'-CAACAAACAAACAAATGC-3' and the second round primers 5'-GAATTCATGGACGGGGCGCCGGTGGCG-3' (EcoRI) with 5'-GGATCC CTAGTACCGGATGTTTGGGTT-3' (BamHI). The *OsMPK5* coding sequence was then cloned in frame to the EcoRI and BamHI sites of the pGADT7 and pGBKT7 vectors, respectively. The complete *OsbZIP60* (Os06g0622700) coding sequence was amplified from mRNA by nested-PCR using the first round primers 5'-CATGGATGTAGAGT TCTTCG-3' with 5'-AGACTGGAAACAACTTTGC-3' and the second round primers 5'-CGGAATTCATGGATGTAGAGTTCT-3' (EcoRI) with 5'-CGGGATCCCTAGCAAGCAGCTGCT-3' (BamHI). The complete *SDRP* (Os03g0102200) coding sequence was amplified from mRNA using the primers 5'-CGGAATTCATGAGCACCATGAAGT-3' (EcoRI) with 5'-CGGGATCCTCATTC CCTCCATCGG-3' (BamHI). Both were then cloned in frame to the EcoRI and BamHI sites of the pGADT7 vector. At least three independent experiments were performed, and the results of one representative experiment are shown.

The Make Your Own "Mate & Plate ™" Library System (Clonetech) was used for yeast two-hybrid screening. A prey cDNA rice library was constructed by fusing cDNAs with the *GAL4* activation domain in the pGADT7-Rec vector. The yeast strain Y2HGold was transformed with the bait plasmid, and the strain Y187 was transformed with the plasmid DNA of the prey cDNA library, according to the manufacturer's instructions. A total of 5.45×10^6 diploids were screened on DDO plates and the mating efficiency was 5%. A total of 385 clones appearing within 7 days were picked out on TDO plates containing 5 mM 3-AT (3-amino-1,2,4-Triazole) and 20 μg/ml X-α-Gal.

BiFC Analysis

The complete *Bphi008a* (or *tBph8a*) coding sequence was cloned in frame to the XbaI and BamHI site of the pSPYNE vector, and the complete *OsMPK5* coding sequence was cloned in frame to the XbaI and BamHI site of the pSPYCE vector. *Arabidopsis* mesophyll protoplasts isolated from 4-week-old WT plants were cotransfected with constructs expressing Bphi008a-pSPYNE (or tBph8a-pSPYNE) and OsMPK5–pSPYCE by previously described procedures (Yoo et al., 2007). Onion epidermal cells were also bombarded with the same constructs as those used to co-transfect the protoplasts. Finally, the protoplasts (or onion epidermal cells) were imaged using a confocal microscope (FV10-ASW; Olympus).

ACKNOWLEDGMENTS

We thank Zhidan Luo and Zhibiao Ye (Huazhong Agricultural University, China) for measuring ethylene emissions. We also thank Lizhong Xiong (Huazhong Agricultural University, China) and Guozhen Liu (Agricultural University of Hebei, China) for providing the OsMPK5 and the HSP82 protein antibody. This research was supported by grants from the National Natural Science Foundation of China (grant No. 30730062), the National Special Key Project on Functional Genomics and Biochip of China (grant No. 2006AA10A103) and a project from the Ministry of Agriculture of China for transgenic research (grant No. 2008ZX08009-003-001).

LITERATURE CITED

Andersen CL, Jensen JL, Ørntoft TF (2004) Normalization of real-time quantitative reverse transcription-PCR data: A model-based variance estimation approach to identify genes suited for normalization, applied to bladder and colon cancer data sets. Cancer Res **64:** 5245–5250

Asai T, Tena G, Plotnikova J, Willmann MR, Chiu WL, Gomez-Gomez L, Boller T, Ausubel FM, Sheen J (2002) MAP kinase signalling cascade in Arabidopsis innate immunity. Nature **415:** 977-983

Ausubel FM (2005) Are innate immune signaling pathways in plants and animals conserved? Nature Immunology **6:** 973-979

Baldwin IT, Kessler A, Halitschke R (2002) Volatile signaling in plant-plant-herbivore interactions: What is real? Curr Opin Plant Biol **5:** 351–354

Berrocal-Lobo M, Molina A, Solano R (2002) Constitutive expression of ETHYLENE-RESPONSE-FACTOR1 in Arabidopsis confers resistance to several necrotrophic fungi. Plant J **29:** 23-32

Brown JK, Czosnek H (2002) Whitefly transmission of plant viruses. In Advances in Botanical Research **36:** 65–100

Chen H, Wilkerson CG, Kuchar JA, Phinney BS, Howe GA (2005) Jasmonate-inducible plant enzymes degrade essential amino acids in the herbivore midgut. Proc Natl Acad Sci USA **102:** 19237–19242

Cheong YH, Moon BC, Kim JK, Kim CY, Kim MC, Kim IH, Park CY, Kim JC, Park BO, Koo SC, Yoon HW, Chung WS, Lim CO, Lee SY, Cho MJ (2003) BWMK1, a rice mitogen-activated protein kinase, locates in the nucleus and mediates pathogenesis-related gene expression by activation of a transcription factor. Plant Physiol **132:** 1961-1972

Chisholm ST, Coaker G, Day B, and Staskawicz BJ (2006) Host-microbe interactions: shaping the evolution of the plant immune response. Cell **124:** 803-814

Du B, Zhang W, Liu B, Hu J, Wei Z, Shi Z, He R, Zhu L, Chen R, Han B, and He G (2009) Identification and characterization of *Bph14*, a gene conferring resistance to brown planthopper in rice. Proc Natl Acad Sci USA **106:** 22163-22168

Farmer EE, Alme´ras E, Krishnamurthy V (2003) Jasmonates and related oxylipins in

plant responses to pathogenesis and herbivory. Curr Opin Plant Biol **6:** 372–378.

Flor HH (1971) Current status of the gene-for-gene concept. Annu Rev Phytopathol **9:** 275–296

Freund C, Dotsch V, Nishizawa K, Reinherz EL, Wagner G (1999) The GYF domain is a novel structural fold that is involved in lymphoid signaling through proline-rich sequences. Nat Struct Biol **6:** 656–660

Glazebrook J (2005) Contrasting mechanisms of defense against biotrophic and necrotrophic pathogens. Annu Rev Phytopathol **43:** 205–227

Guo H, Ecker JR (2004) The ethylene signaling pathway: new insights. Curr Opin in Plant Biol **7:** 40–49

Gutterson N, Reuber TL (2004) Regulation of disease resistance pathways by AP2/ERF transcription factors. Curr Opin in Plant Biol **7:** 465–471

Hamel LP, Nicole MC, Sritubtim S, Morency MJ, Ellis M, Ehlting J (2006) Ancient signals: Comparative genomics of plant MAPK and MAPKK gene families. Trends Plant Sci **11:** 192−198

Hao P, Liu C, Wang Y, Chen R, Tang M, Du B, Zhu L, He G (2008) Herbivore-induced callose deposition on the sieve plates of rice: An important mechanism for host resistance. Plant Physiol **146:** 1810-1820

He P, Shan L, Lin NC, Martin GB, Kemmerling B, Nürnberger T, Sheen J (2006) Specific bacterial suppressors of MAMP signaling upstream of MAPKKK in Arabidopsis innate immunity. Cell **125:** 563-575

Hellemans J, Mortier G, De Paepe A, Speleman F, Vandesompele J (2007) qBase relative quantification framework and software for management and automated analysis of real-time quantitative PCR data. Genome Biology **8:** 19.1-19.14

Hiei Y, Ohta S, Komari T, Kumashiro T (1994) Efficient transformation of rice (*Oryza sativa* L.) mediated by *Agrobacterium* and sequence analysis of the boundaries of the T-DNA. Plant J **6:** 271–282

Howe GA, Jander G (2008) Plant immunity to insect herbivores. Annu Rev Plant Biol **59:** 41–66

Huang Z, He G, Shu L, Li X, Zhang Q (2001) Identification and mapping of two brown planthopper resistance genes in rice. Theor Appl Genet **102:** 929-934

Iwai T, Miyasaka A, Seo S, Ohashi Y (2006) Contribution of ethylene biosynthesis for resistance to blast fungus infection in young rice plants. Plant Physiol **142:** 1202–1215

Iwata Y, Koizumi N (2005) An Arabidopsis transcription factor, AtbZIP60, regulates the endoplasmic reticulum stress response in a manner unique to plants. Proc Natl Acad Sci USA **102:** 5280-5285

Iwata Y, Fedoroff NV, Koizumi N (2008) Arabidopsis bZIP60 is a proteolysis-activated transcription factor involved in the endoplasmic reticulum stress response. Plant Cell **20:** 3107–3121

Iwata Y, Yoneda M, Yanagawa Y, Koizumi N (2009) Characteristics of the nuclear form of the Arabidopsis transcription factor AtbZIP60 during the endoplasmic reticulum stress response. Biosci Biotechnol Biochem **73:** 865-869

Jonak C, Okresz L, Bogre L, Hirt H (2002) Complexity, cross talk and integration of plant MAP kinase signalling. Curr Opin Plant Biol **5:** 415−424

Jones JDG, Dangl JL (2006) The plant immune system. Nature **444:** 323-329

Kaloshian I, Walling LL (2005) Hemipterans as plant pathogens. Annu Rev Phytopathol **43:** 491–521

Kandoth PK, Ranf S, Pancholi SS, Jayanty S, Walla MD, Miller W, Howe GA, Lincoln DE, Stratmann JW (2007) Tomato MAPKs LeMPK1, LeMPK2, and LeMPK3 function in the systemin-mediated defense response against herbivorous insects. Pro Nat Aca Sci USA **104:** 12205–12210

Kay BK, Williamson MP, Sudol M (2000) The importance of being proline: the interaction of proline-rich motifs in signaling proteins with their cognate domains. FASEB **14:** 231-241

Kempema LA, Cui X, Holzer FM, Walling LL (2007) Arabidopsis transcriptome changes in response to phloem-feeding silverleaf whitefly nymphs. Similarities and distinctions in responses to aphids. Plant Physiol **143:** 849–865

Kendrick MD, Chang C (2008) Ethylene signaling: new levels of complexity and regulation. Curr Opin in Plant Biol **11:** 1–7

Kofler MM, Freund C (2006) The GYF domain. FEBS Journal **273:** 245–256

Lorenzo O, Piqueras R, Sanchez-Serrano JJ, Solano R (2003) ETHYLENE

RESPONSE FACTOR1 Integrates Signals from Ethylene and Jasmonate Pathways in Plant Defense. Plant Cell **15:** 165–178

Maffei ME, Mithöfer A, Boland W (2007) Before gene expression: early events in plant insect interaction. Trends Plant Sci **12:** 310–316

Mizoguchi T, Irie K, Hirayama T, Hayashida N, Yamaguchi-shinozaki K, Matsumoto K, Shiozaki K (1996) A gene encoding a mitogen-activated protein kinase kinase kinase is induced simultaneously with genes for a mitogen-activated protein kinase and S6 ribosomal protein kinase by touch, cold and water stress in Arabidopsis thaliana. Pro Natl Acad Sci USA **93:** 765-769

Musser RO, Hum-Musser SM, Eichenseer H, Peiffer M, Ervin G (2002) Herbivory: Caterpillar saliva beats plant defences - a new weapon emerges in the evolutionary arms race between plants and herbivores. Nature **416:** 599–600

Obenauer JC, Cantley LC, Yaffe MB (2003) Scansite 2.0: proteome-wide prediction of cell signaling interactions using short sequence motifs. Nucleic Acids Res **31:** 3635–3641

Pitzschke A, Schikora A, Hirt H (2009) MAPK cascade signalling networks in plant defence. *Curr Opin in Plant Biol* **12:** 1-6

Ptacek, J., Devgan, G., Michaud, G., Zhu, H., Zhu, X., Fasolo, J., Guo, H., Jona, G., Breitkreutz, A., Sopko, R., et al (2005) Global analysis of protein phosphorylation in yeast. Nature **438:** 679-684

Puntervoll P, Linding R, Gemund C, Chabanis-Davidson S, Mattingsdal M, Cameron S, Martin D, Ausiello G, Brannetti B, Costantini A (2003) ELM server: a new resource for investigating short functional sites in modular eukaryotic proteins. Nucleic Acids Res **31:** 3625–3630

Ren D, Liu Y, Yang KY, Han L, Mao G, Glazebrook J, Zhang S (2008) A fungal-responsive MAPK cascade regulates phytoalexin biosynthesis in Arabidopsis. Proc Natl Acad Sci USA **105:** 145638-145643.

Reyna NS, Yang Y (2006) Molecular analysis of the rice MAP kinase gene family in relation to *Magnaporthe grisea* infection. Mol Plant Microbe Interact **19:** 530–540

Rossi M, Goggin FL, Milligan SB, Kaloshian I, Ullman DE, Williamson VM (1998) The nematode resistance gene *Mi* of tomato confers resistance against the potato

aphid. Proc Natl Acad Sci USA **95:** 9750-9754

Scheideler M, Schlaich NL, Fellenberg K, Beissbarth T, Hauser NC, Vingron M, Slusarenko AJ, Hoheisel JD (2002) Monitoring the switch from housekeeping to pathogen defense metabolism in *Arabidopsis thaliana* using cDNA array. J Biol Chem **277:** 10555-10561.

Schmittgen TD, Livak KJ (2008) Analyzing real-time PCR data by the comparative C_T method. Nature Protocols **3:** 1101-1108

Schmittgen TD, Zakrajsek BA (2000) Effect of experimental treatment on housekeeping gene expression: validation by real-time, quantitative RT-PCR. *J Biochem Biophys* Methods **46:** 69–81

Takahashi F, Yoshida R, Ichimura K, Mizoguchi T, Seo S, Yonezawa M, Maruyama K, Yamaguchi-Shinozaki K, Shinozaki K (2007) The mitogen-activated protein kinase cascade MKK3-MPK6 is an important part of the jasmonate signal transduction pathway in Arabidopsis. Plant Cell **19:** 805-818

Tateda C, Ozaki R, Onodera Y, Takahashi Y, Yamaguchi K, Berberich T, Koizumi N, Kusano T (2008) NtbZIP60, an endoplasmic reticulum-localized transcription factor, plays a role in the defense response against bacterial pathogens in *Nicotiana tabacum*. J Plant Res **121:** 603–611

Tjallingii WF (2006) Salivary secretions by aphids interacting with proteins of phloem wound responses. J Exp Bot **57:** 739-745

Ussuf KK, Laxmi NH, Mitra R (2001) Proteinase inhibitors: plant-derived genes of insecticidal protein for developing insect-resistant transgenic plants. Curr Sci **80:** 847–853

Vandesompele J, De Preter K, Pattyn F, Poppe B, Van Roy N, De Paepe A, Speleman F (2002) Accurate normalization of real-time quantitative RT-PCR data by geometric averaging of multiple internal control genes. Genome Biology **3:** 0034.1-0034.12

Voelckel C, Baldwin IT (2004) Herbivore-induced plant vaccination. Part II. Array-studies reveal the transience of herbivore-specific transcriptional imprints and a distinct imprint from stress combinations. Plant J **38:** 650 – 663

Walter M, Chaban C, Schütze K, Batistic O, Weckermann K, Näke C, Blazevic D,

Grefen, C, Schumacher K, Oecking C, Harter K, Kudla J (2004) Visualization of protein interactions in living plant cells using bimolecular fluorescence complementation. Plant J **40:** 428-438

Wang YY, Wang XL, Yuan HY, Chen RZ, Zhu LL, He RF, He GC (2008) Responses of two contrasting genotypes of rice to brown planthopper. Mol Plant Microbe Interact **20:** 122-132

Wei Z, Hu W, Lin QS, Cheng XY, Tong MJ, Zhu LL, Chen RZ, He GC (2009) Understanding rice plant resistance to the Brown Planthopper (*Nilaparvata lugens*): A proteomic approach. Proteomics **9:** 2798-2808

Wesley SV, Helliwell CA, Smith NA, Wang MB, Rouse DT, Liu Q, Gooding PS, Singh SP, Abbott D, Stoutjesdijk PA (2001) Construct design for efficient, effective and high-throughput gene silencing in plants. Plant J **27:** 581–590

Will T, Tjallingii WF, Tho¨nnessen A, Bel A (2007) Molecular sabotage of plant defense by aphid saliva. Proc Natl Acad Sci USA **104:** 10536–10541

Wu J, Hettenhausen C, Meldau S, Baldwin IT (2007) Herbivory rapidly activates MAPK signaling in attacked and unattacked leaf regions but not between leaves of *Nicotiana attenuata*. Plant Cell **19:** 1096–1122

Xiong L, Yang Y (2003) Disease resistance and abiotic stress tolerance in rice are inversely modulated by an abscisic acid-inducible mitogen-activated protein kinase. Plant Cell **15:** 745-759

Yang SF, Hoffman NE (1984) Ethylene biosynthesis and its regulation in higher plants. Ann Rev Plant Physiol **35:** 155-189

Yoo SD, Cho YH, Sheen J (2007) *Arabidopsis* mesophyll protoplasts: a versatile cell system for transient gene expression analysis. Nature Protocols **2:** 1565-1572

Yoo SD, Cho YH, Tena G, Xiong Y, Sheen J (2008) Dual control of nuclear EIN3 by bifurcate MAPK cascades in C_2H_4 signalling. Nature **451:** 789-796

Yuan H, Chen X, Zhu L, He G (2004) Isolation and characterization of a novel rice gene encoding a putative insect-inducible protein homologous to wheat Wir1. J of Plant Physiol **161:** 79–85

Zarate SI, Kempema LA, Walling LL (2007) Silverleaf whitefly induces salicylic acid defenses and suppresses effectual jasmonic acid defenses. Plant Physiol **143:**

866–875

Zhou N, Tootle TL, Tsui F, Klessig DF, Glazebrook J (1998) PAD4 functions upstream from salicylic acid to control defense responses in Arabidopsis. Plant Cell **10:**1021–30

Zhu-Salzman K, Salzman RA, Ahn JE, Koiwa H (2004) Transcriptional regulation of sorghum defense determinants against a phloem-feeding aphid. Plant Physiol **134:** 420–431

FIGURE LEGENDS

Figure 1. Northern and Southern-blot analysis of *Bphi008a* in WT and transgenic plants, and evaluation of its contribution to resistance to the BPH. **A**, *Bphi008a* expression levels in normal WT and six T0 OE plants. OE17 was a three-copy insertion plant, OE10 was a two-copy insertion plant and the rest were one-copy insertion plants. **B**, *Bphi008a* expression levels in normal WT and six T0 RNAi plants after the BPH had been feeding for 48 h. **C**, Southern-blot analysis of OE21 T2 progeny. 1-6, samples from six randomly chosen T2 plants; M, λDNA/Hind III marker. **D**, Evaluation of resistance to the BPH. Fifty plants of each line were chosen for analysis of percentage of severity score to BPH after the BPH had been feeding for 72, 96 and 120 h. Five independent experiments were performed with similar results, and the results of one representative experiment are shown. **E**, EPG evaluation of BPH phloem-feeding times on OE10, OE21, WT, RNAi5 and RNAi7 plants. Each bar represents the mean time ±SE of five replicates. **F**, Honeydew area evaluation after the BPH had been feeding for 48 and 72 h on OE21 and WT plants. The size of the honeydew area and the intensity of the honeydew color indicate the BPH feeding activity. Standard bars (SBs) indicate mean values from eight replicates. Significant differences in **E** and **F** are indicated with *(P<0.05) or **(P<0.01); Student's *t* test.

Figure 2. Determination of the optimal numbers of control genes for normalization. Average expression stability values (M) of the remaining HK genes during stepwise exclusion of the least stably expressed HK gene in leaf-sheath cDNA-samples after BPH-feeding for 0, 6, 12, 24, 48, 72 and 96 h. **A**, HK genes stability evaluation and choice in WT lines. **B**, HK genes stability evaluation and choice in OE and control WT lines. **C**, HK genes stability evaluation and choice in RNAi and control WT lines. **D**, HK genes stability evaluation and choice in 1-MCP treated WT and control WT lines. **E**, Pairwise variation ($V_{n/n+1}$) analysis between the normalization factors NF_n and NF_{n+1} to determine the number of control genes required for accurate normalization in our study. This experiment was repeated with two biological replicates and we obtained the same results.

Figure 3. *Bphi008a* is a downstream gene of the ethylene signaling pathway. **A** and **B**, Comparative expression levels of members of the *OsACS* and *OsACO* family after BPH-feeding for between 0 h and 96 h on WT plants. **C**, Profiles of ethylene emissions from WT plants after BPH-feeding for between 3 h and 72 h. Values shown are means ± SD based on three independent experiments. The experiment was repeated two times with similar results. **D**, *Bphi008a* expression patterns with and without 1-MCP treatment in response to BPH-feeding from 0 h to 96 h on Hejiang 19 plants.

Figure 4. *Bphi008a* expression patterns in rice from the seedling and heading stages (the HK gene used for normalization in this study was *LSD1*).

Figure 5. Subcellular localization of *Bphi008a*, *tnBph8a* and *OsMPK5*. **A**, YFP protein localization in onion epidermal cells. **B** and **C**, YFP-tnBph8a fusion protein localization in onion epidermal cells. **D**, Dual YFP-Bphi008a protein localization in onion epidermal cells. **E**, Dual YFP-OsMPK5 protein localization in onion epidermal cells. Scale bar = 50 μm.

Figure 6. Bphi008a interacts with OsMPK5 *in vitro* and *in vivo*. **A**, Possible motifs of the Bphi008a protein. Enclosed squares are two possible Pro-X-X-Pro motifs and one Pro-Pro-Gly-Arg motif. Bold black, prolines in possible motifs; Red, possible Thr phosphorylated sites before the Pro-X-X-Pro motifs; Blue, positively charged Arg in motifs. The shadowed region of the C-terminal was also cleaved and the remaining region was used as a negative control. **B** and **C**, Phosphorylation of the Bphi008a by OsMPK5 *in vitro*. Lanes 1-6: kinase activities obtained from incubating 3 μg of GST-Bphi008a protein with 0.5, 1, 2, 4 8 and 16 μg of GST-OsMPK5 protein, respectively, in an *in vitro* assay. Lanes 7-8: kinase activities obtained from incubating 3 μg GST or GST-tBph8a protein, respectively, with 16 μg of GST-OsMPK5 protein in an *in vitro* assay. M: protein masses in KD. **D**, Yeast two-hybrid assay of the interaction between Bphi008a or tBph8a and OsMPK5. The diploids were grown in DDO plates, and transferred to QDO/X-α-Gal/3-AT plates with 20 μg/ml X-α-Gal and 10 μM 3-AT (3-amino-1,2,4-Triazole) for 3 days. **E**, Relative *β*-galactosidase activities obtained were

consistent with the results observed in QDO/X-α-Gal /3-AT plates. **F**, BiFC visualization of the Bphi008a-OsMPK5 and tBph8a-OsMPK5 interaction in transiently coexpressed Arabidopsis mesophyll protoplasts. The *pBS-35S-YFP* vector served as a transfected control, and the Arabidopsis nuclear protein bZIP63 served as a BiFC positive control. Scale bar = 10 μm.

Figure 7. *OsMPK5*, *OsMPK12*, *OsMPK13* and *OsMPK17* expression patterns in transgenic and WT plants after the BPH had been feeding for between 0 h and 96 h (corresponding *Bphi008a* expression levels in transgenic and WT plants are shown in Supplemental Figure 4).

Figure 8. A, Immunoblot analysis of OsMPK5 in transgenic and WT plants after the BPH had been feeding for between 0 h and 96 h. Protein (50 μg) was separated by SDS-PAGE, electroblotted, and probed with rabbit OsMPK5 polyclonal antibody (1:1000). After incubation with goat anti-rabbit IgG (1:10000) conjugated to alkaline phosphatase, the complex was visualized using BCIP/NBT solution. Rice HSP82 (Q69QQ6) mouse monoclonal antibody (1:10000) was used as a loading control. **B**, Comparative protein levels of OsMPK5 in WT and transgenic plants from three replicates. The Western-blot signals of OsMPK5 were analyzed with 'Quantity One' (Bio-Rad) and showed with histogram. **C** to **G**, Comparative expression levels of *OsERF1*, *OsEREBP1*, *Arginase*, *LEA2* and *CysPI* after the BPH had been feeding for between 0 h and 96 h in WT and transgenic plants. Each bar represents the mean values ±SE of three replicates. Significant differences in **B** to **G** are indicated with *(P<0.05) or **(P<0.01); Student's *t* test.

Figure 9. Bphi008a-interacting proteins identified by yeast two-hybrid screening and its interaction with OsbZIP60 or SDRP *in vivo*. **A**, Bphi008a-interacting proteins identified by yeast two-hybrid screening. The Bphi008a-interacting proteins were classified into five categories (as indicated in frame boxes) based on their putative functions. **B**, Yeast two-hybrid assay of the interaction between Bphi008a and OsbZIP60 or SDRP.

TDO/3-AT plates containing 5 mM 3-AT (3-amino-1,2,4-Triazole); QDO/X-α-Gal/3-AT plates containing 10 mM 3-AT and 20 μg/ml X-α-Gal. **C**, Comparative expression levels of *OsbZIP60* after the BPH had been feeding for between 0 h and 96 h in WT and transgenic plants.

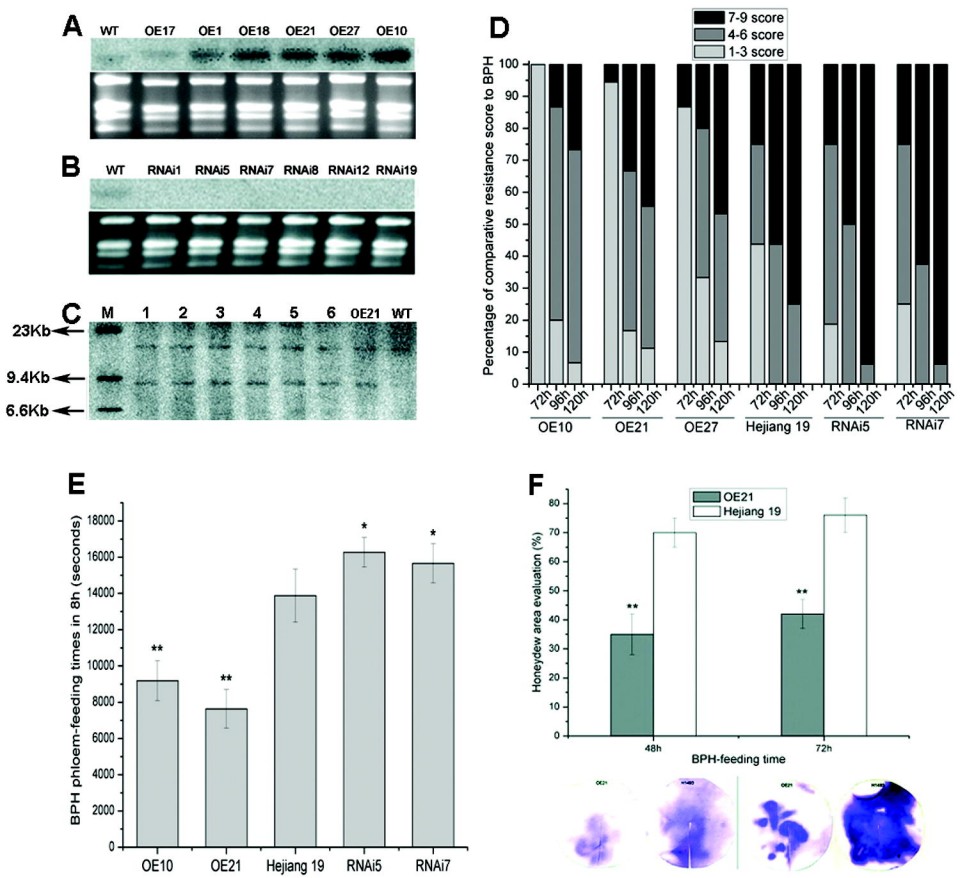

Figure 1. Northern and Southern-blot analysis of *Bphi008a* in WT and transgenic plants, and evaluation of its contribution to resistance to the BPH. **A**, *Bphi008a* expression levels in normal WT and six T0 OE plants. OE17 was a three-copy insertion plant, OE10 was a two-copy insertion plant and the rest were one-copy insertion plants. **B**, *Bphi008a* expression levels in normal WT and six T0 RNAi plants after the BPH had been feeding for 48 h. **C**, Southern-blot analysis of OE21 T2 progeny. 1-6, samples from six randomly chosen T2 plants; M, λDNA/Hind III marker. **D**, Evaluation of resistance to the BPH. Fifty plants of each line were chosen for analysis of percentage of severity score to BPH after the BPH had been feeding for 72, 96 and 120 h. Five independent experiments were performed with similar results, and the results of one representative experiment are shown. **E**, EPG evaluation of BPH phloem-feeding times on OE10, OE21, WT, RNAi5 and RNAi7 plants. Each bar represents the mean time ±SE of five replicates. **F**, Honeydew area evaluation after the BPH had been feeding for 48 and 72 h on OE21 and WT plants. The size of the honeydew area and the intensity of the honeydew color indicate the BPH feeding activity. Standard bars (SBs) indicate mean values from eight replicates. Significant differences in **E** and **F** are indicated with *(P<0.05) or **(P<0.01); Student's t test.

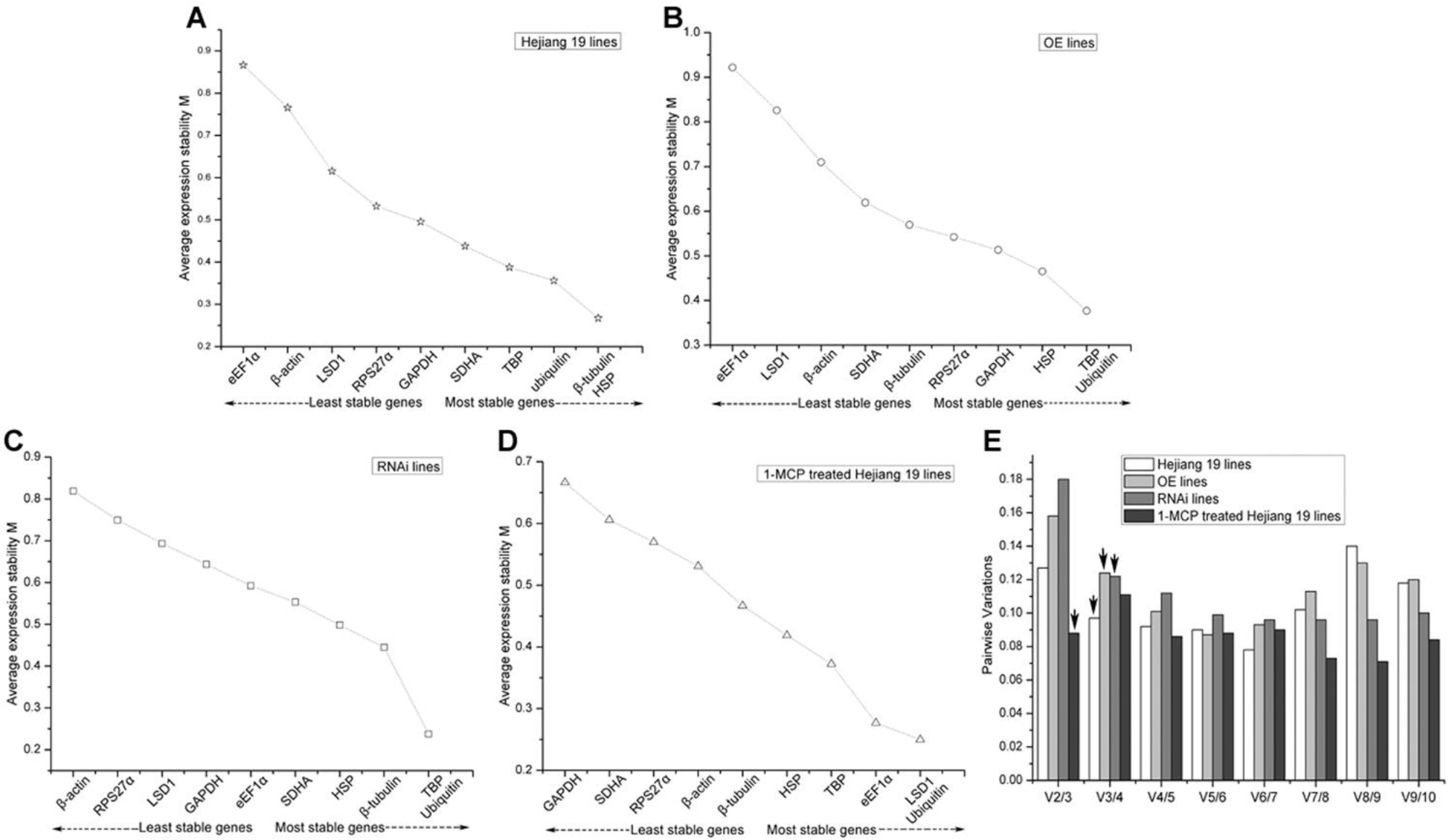

Figure 2. Determination of the optimal numbers of control genes for normalization. Average expression stability values (M) of the remaining HK genes during stepwise exclusion of the least stably expressed HK gene in leaf-sheath cDNA-samples after BPH-feeding for 0, 6, 12, 24, 48, 72 and 96 h. **A**, HK genes stability evaluation and choice in WT lines. **B**, HK genes stability evaluation and choice in OE and control WT lines. **C**, HK genes stability evaluation and choice in RNAi and control WT lines. **D**, HK genes stability evaluation and choice in 1-MCP treated WT and control WT lines. **E**, Pairwise variation ($V_{N/N+1}$) analysis between the normalization factors NF_N and NF_{N+1} to determine the number of control genes required for accurate normalization in our study. This experiment was repeated with two biological replicates and we obtained the same results.

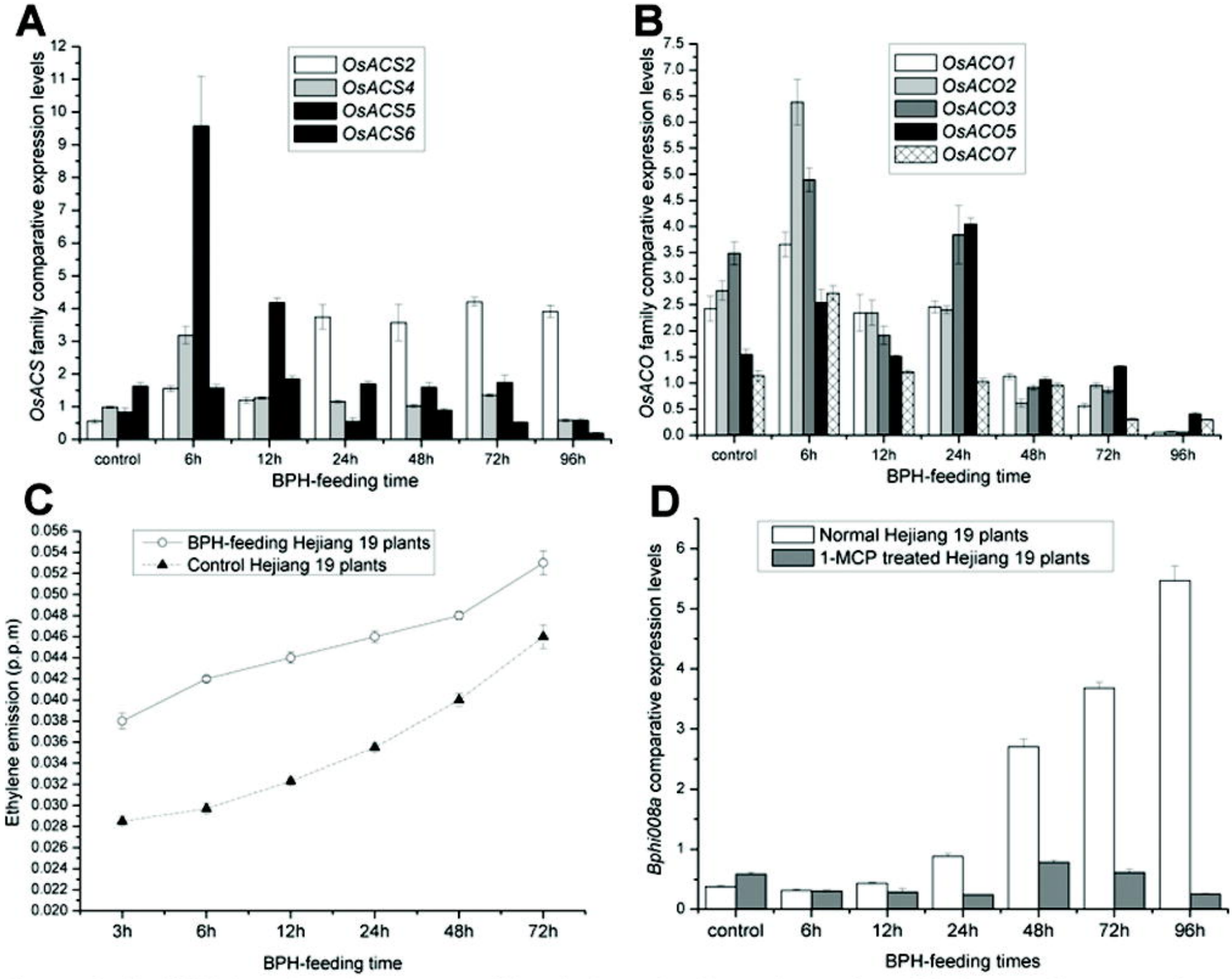

Figure 3. *Bphi008a* is a downstream gene of the ethylene signaling pathway. **A** and **B**, Comparative expression levels of members of the *OsACS* and *OsACO* family after BPH-feeding for between 0 h and 96 h on WT plants. **C**, Profiles of ethylene emissions from WT plants after BPH-feeding for between 3 h and 72 h. Values shown are means ±SD based on three independent experiments. The experiment was repeated two times with similar results. **D**, *Bphi008a* expression patterns with and without 1-MCP treatment in response to BPH-feeding from 0 h to 96 h on Hejiang 19 plants.

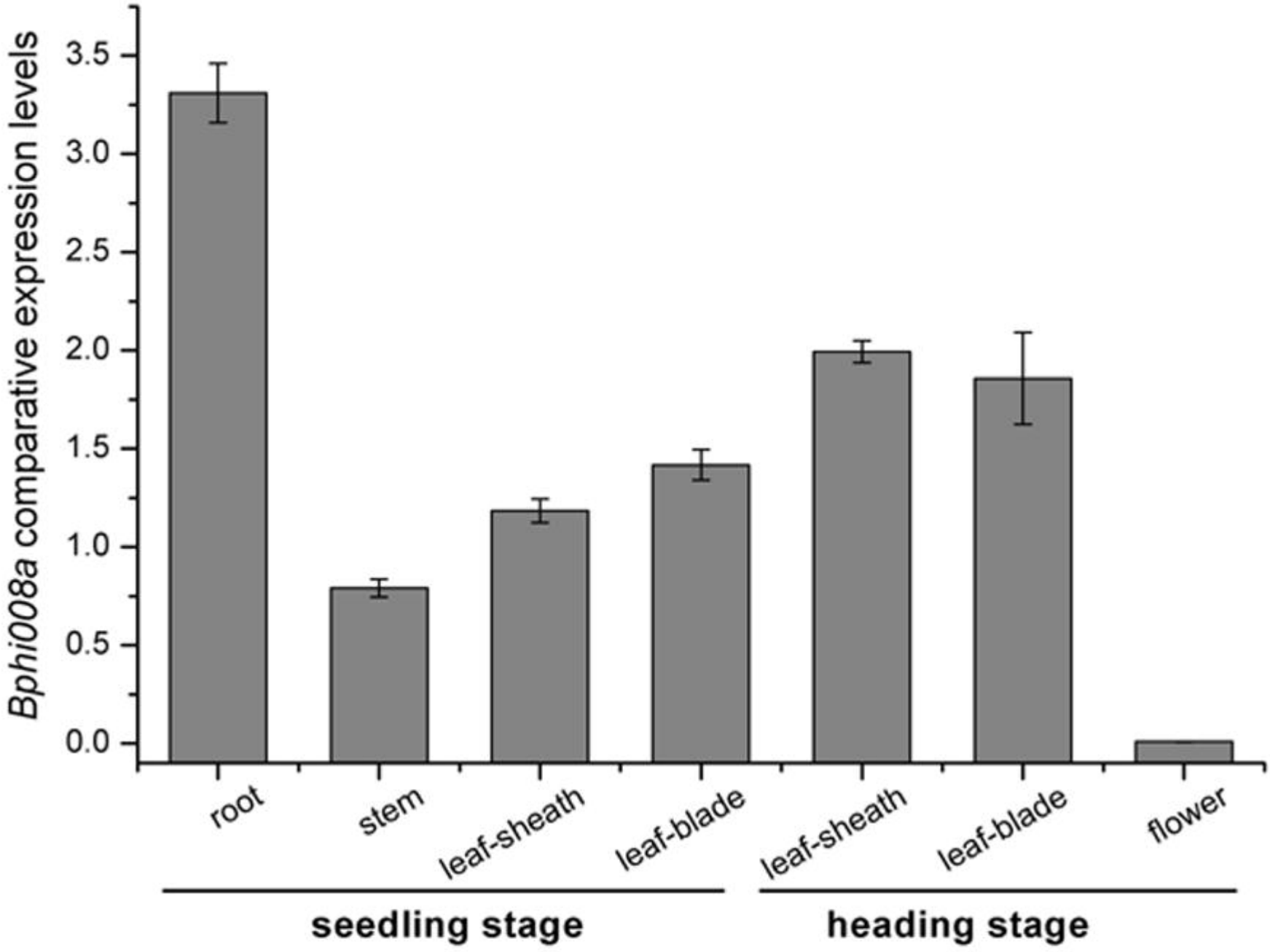

Figure 4. *Bphi008a* expression patterns in rice from the seedling and heading stages (the HK gene used for normalization in this study was *LSD1*).

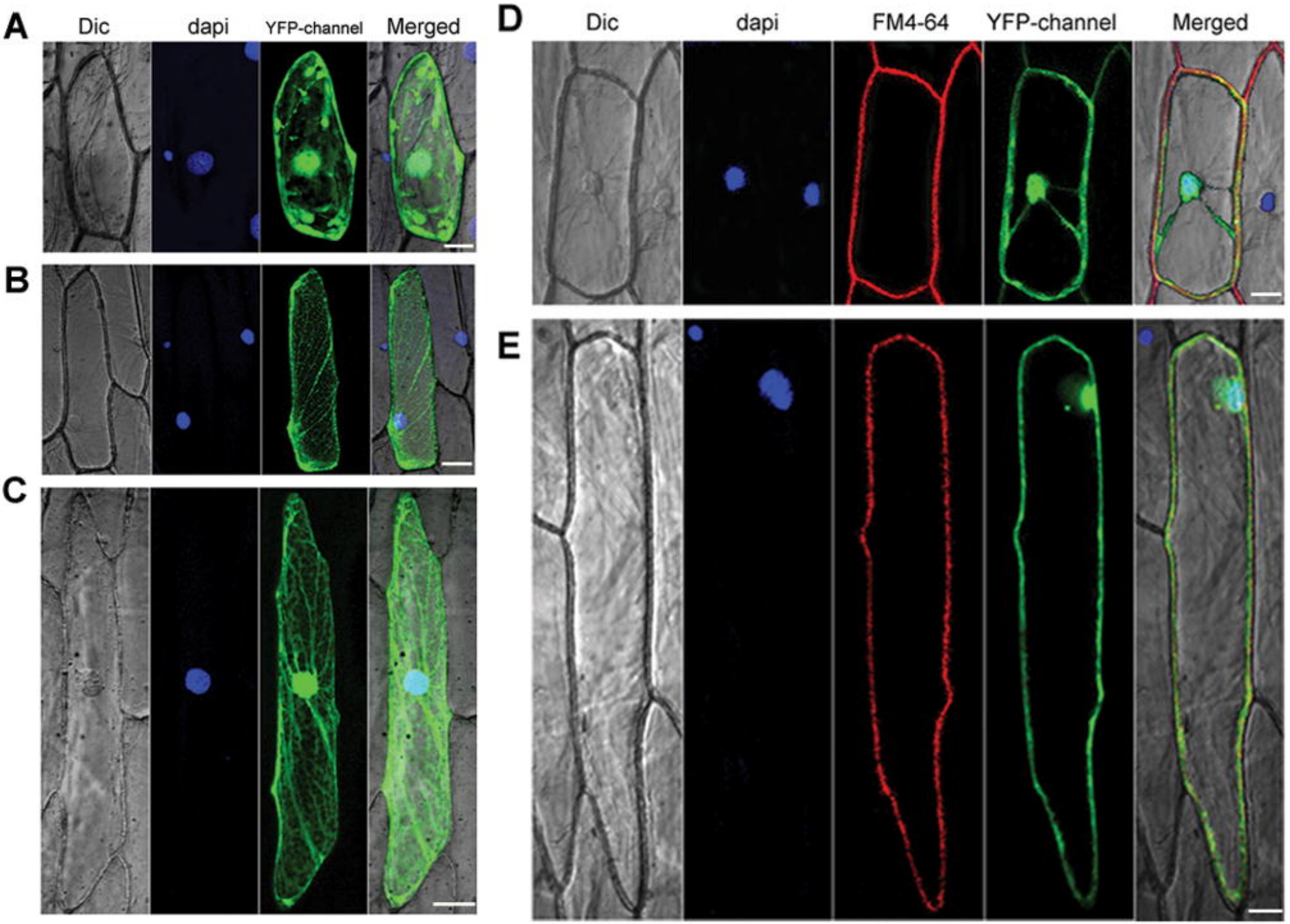

Figure 5. Subcellular localization of *Bphi008a*, *tnBph8a* and *OsMPK5*. **A**, YFP protein localization in onion epidermal cells. **B** and **C**, YFP-tnBph8a fusion protein localization in onion epidermal cells. **D**, Dual YFP-Bphi008a protein localization in onion epidermal cells. **E**, Dual YFP-OsMPK5 protein localization in onion epidermal cells. Scale bar = 50 μm.

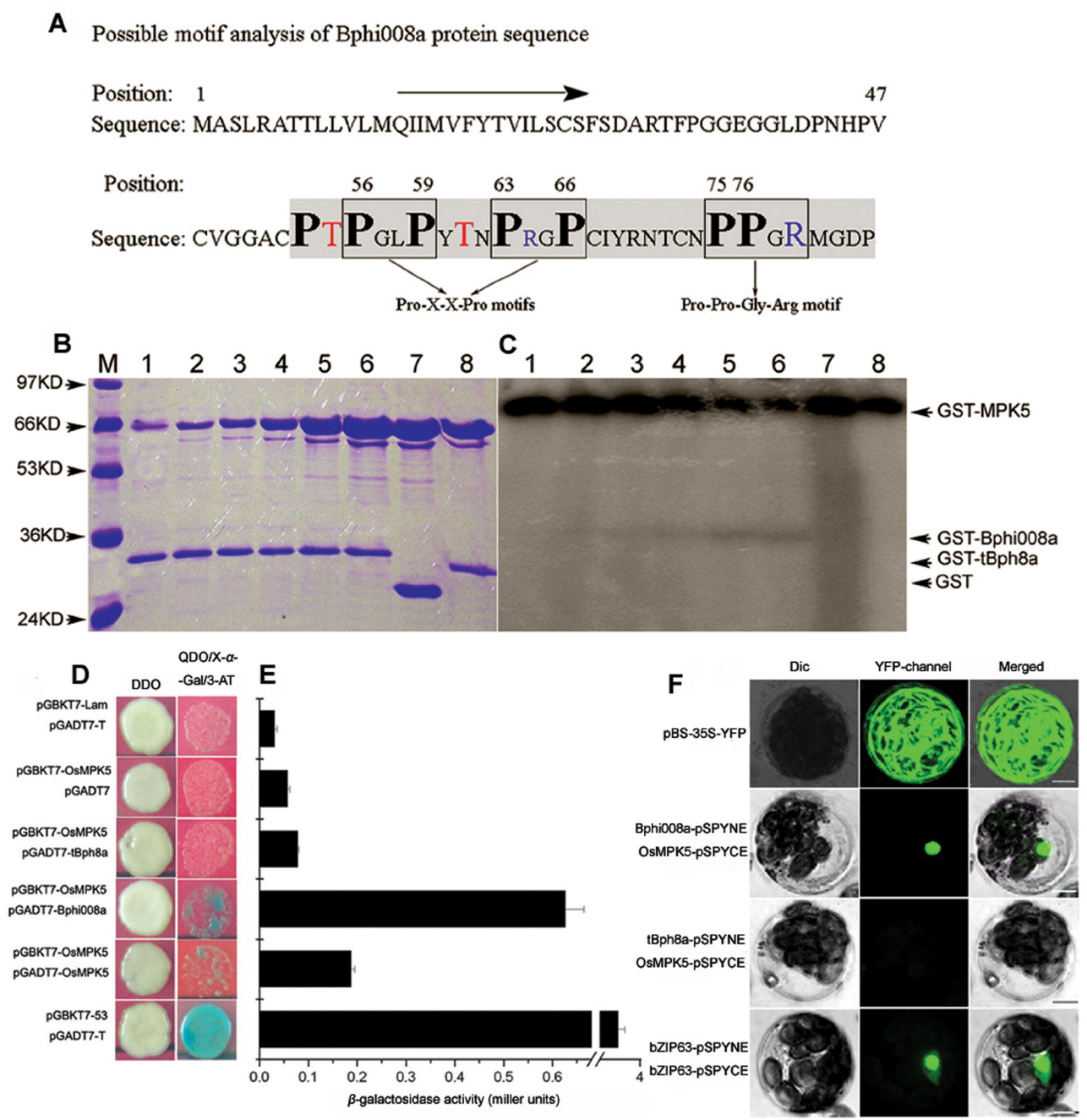

Figure 6. Bphi008a interacts with OsMPK5 *in vitro* and *in vivo*. **A**, Possible motifs of the Bphi008a protein. Enclosed squares are two possible Pro-X-X-Pro motifs and one Pro-Pro-Gly-Arg motif. Bold black, prolines in possible motifs; Red, possible Thr phosphorylated sites before the Pro-X-X-Pro motifs; Blue, positively charged Arg in motifs. The shadowed region of the C-terminal was also cleaved and the remaining region was used as a negative control. **B** and **C**, Phosphorylation of the Bphi008a by OsMPK5 *in vitro*. Lanes 1-6: kinase activities obtained from incubating 3 μg of GST-Bphi008a protein with 0.5, 1, 2, 4 8 and 16 μg of GST-OsMPK5 protein, respectively, in an *in vitro* assay. Lanes 7-8: kinase activities obtained from incubating 3 μg GST or GST-tBph8a protein, respectively, with 16 μg of GST-OsMPK5 protein in an *in vitro* assay. M: protein masses in kDa. **D**, Yeast two-hybrid assay of the interaction between Bphi008a or tBph8a and OsMPK5. The diploids were grown in DDO plates, and transferred to QDO/X-α-Gal/3-AT plates with 20 μg/ml X-α-Gal and 10 μM 3-AT (3-amino-1,2,4-Triazole) for 3 days. **E**, Relative *β*-galactosidase activities obtained were consistent with the results observed in QDO/X-α-Gal /3-AT plates. **F**, BiFC visualization of the Bphi008a-OsMPK5 and tBph8a-OsMPK5 interaction in transiently coexpressed Arabidopsis mesophyll protoplasts. The *pBS-35S-YFP* vector served as a transfected control, and the Arabidopsis nuclear protein bZIP63 served as a BiFC positive control . Scale bar = 10 μm.

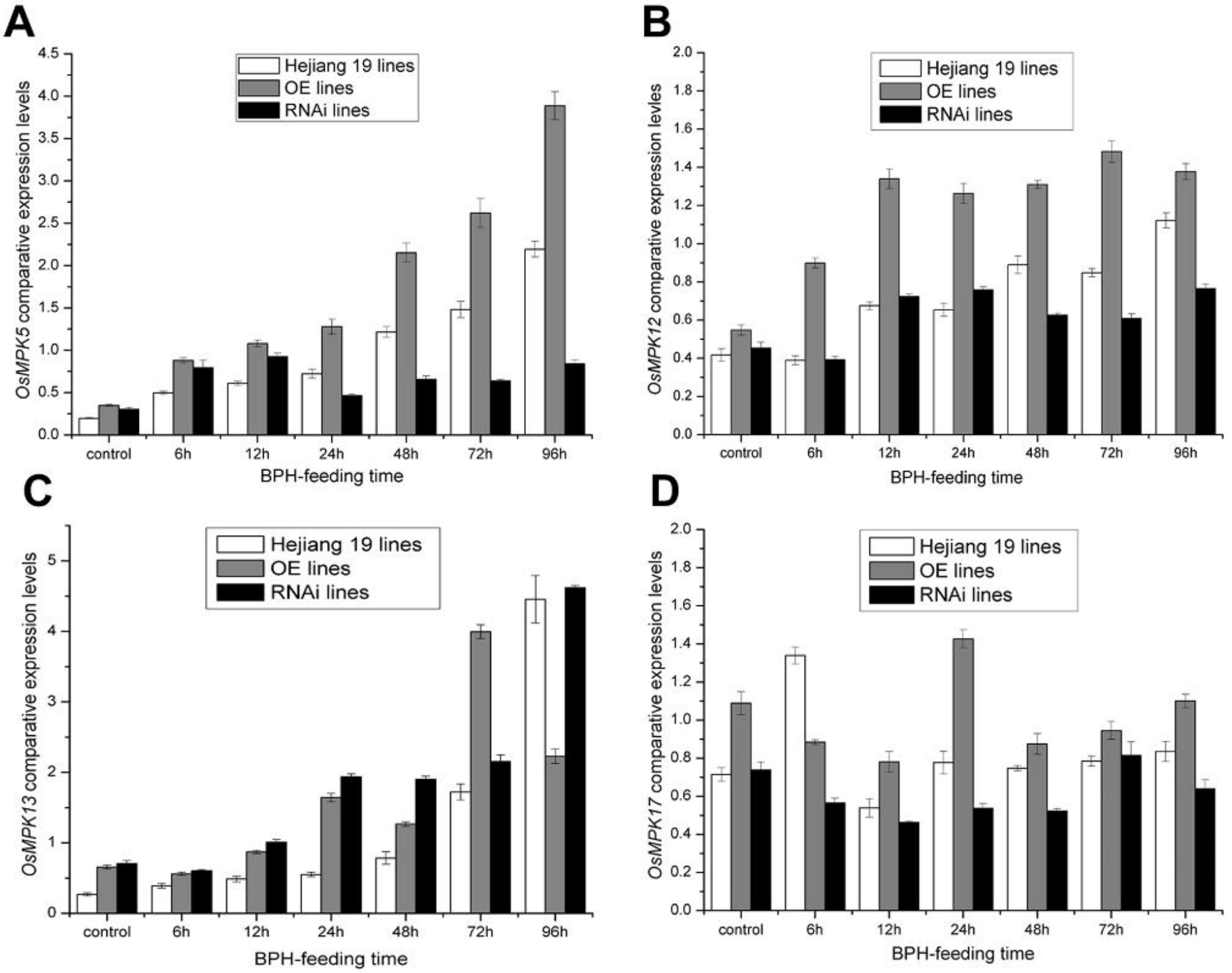

Figure 7. *OsMPK5*, *OsMPK12*, *OsMPK13* and *OsMPK17* expression patterns in transgenic and WT plants after the BPH had been feeding for between 0 h and 96 h (corresponding *Bphi008a* expression levels in transgenic and WT plants are shown in Supplemental Figure 4).

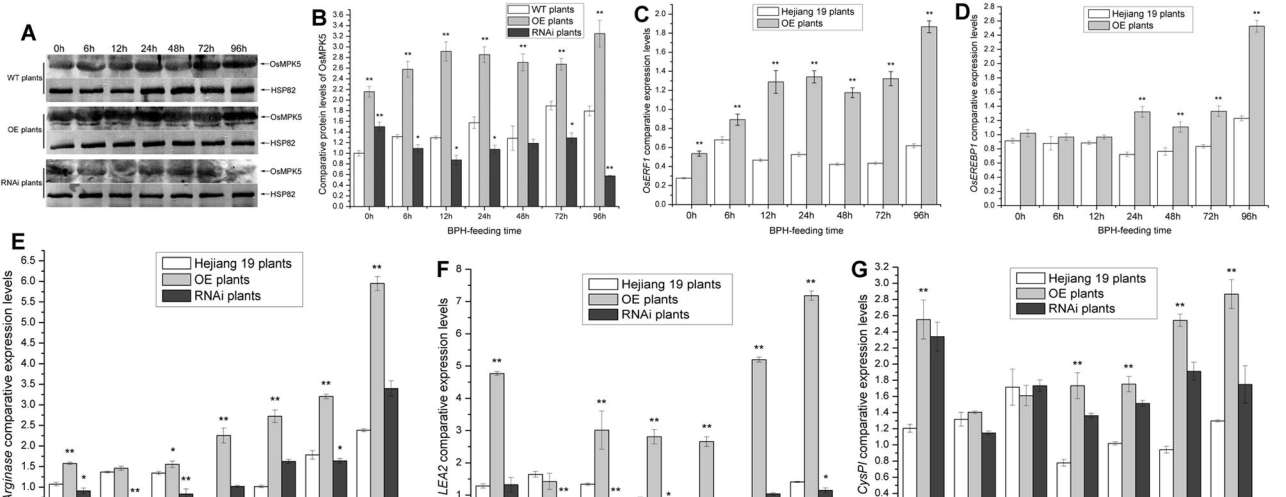

Figure 8. A, Immunoblot analysis of OsMPK5 in transgenic and WT plants after the BPH had been feeding for between 0 h and 96 h. Protein (50 μg) was separated by SDS-PAGE, electroblotted, and probed with rabbit OsMPK5 polyclonal antibody (1:1000). After incubation with goat anti-rabbit IgG (1:10000) conjugated to alkaline phosphatase, the complex was visualized using BCIP/NBT solution. Rice HSP82 (Q69QQ6) mouse monoclonal antibody (1:10000) was used as a loading control. **B**, Comparative protein levels of OsMPK5 in WT and transgenic plants from three replicates. The Western-blot results of OsMPK5 were analyzed with 'Quantity One' (Bio-Rad) and showed with histogram. **C** to **G**, Comparative expression levels of *OsERF1*, *OsEREBP1*, *Arginase*, *LEA2* and *CysPI* after the BPH had been feeding for between 0 h and 96 h in WT and transgenic plants. Each bar represents the mean values ±SE of three replicates. Significant differences in **B** to **G** are indicated with *($P<0.05$) or **($P<0.01$); Student's *t* test.

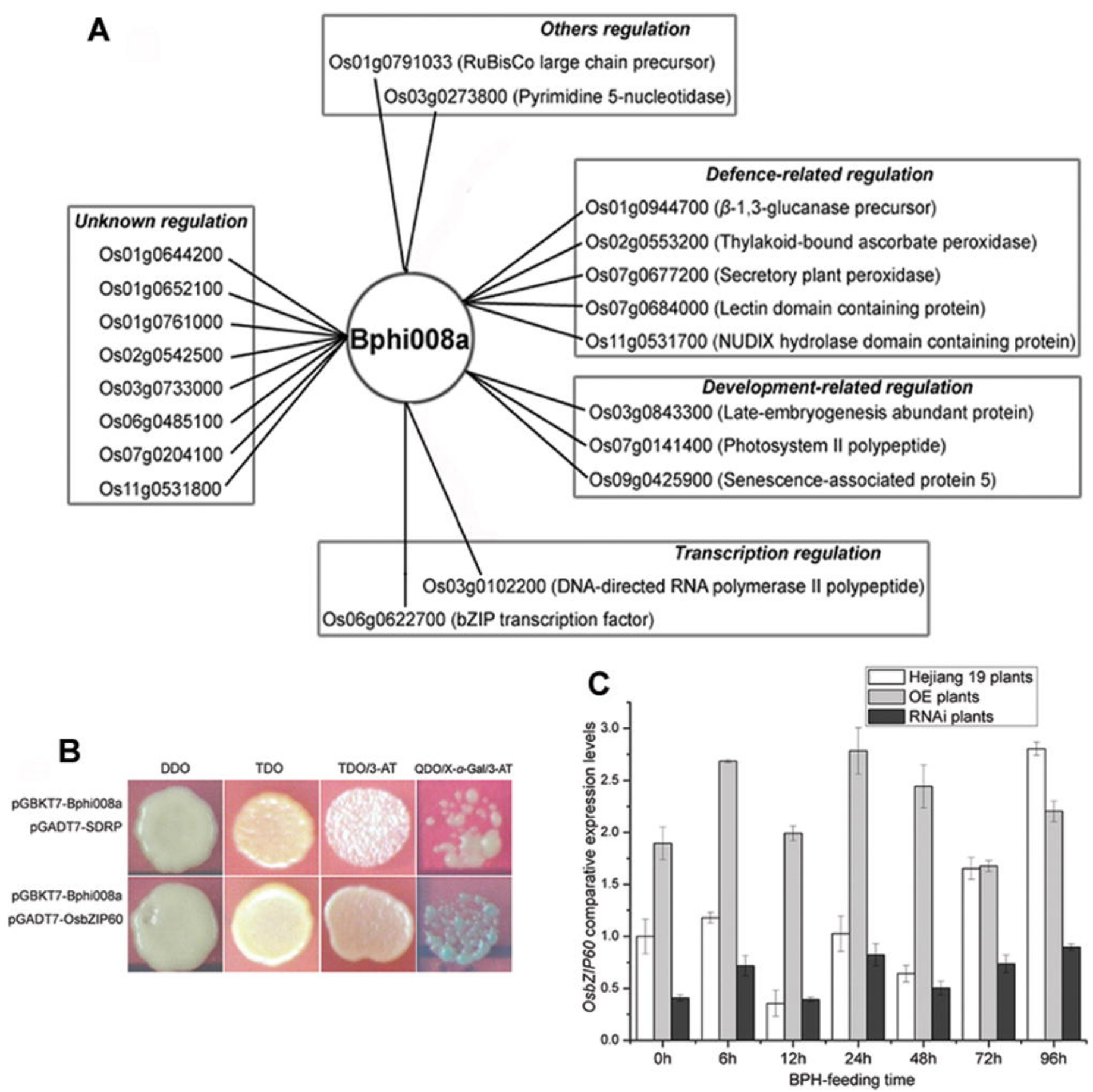

Figure 9. Bphi008a-interacting proteins identified by yeast two-hybrid screening and its interaction with OsbZIP60 or SDRP *in vivo*. **A**. Bphi008a-interacting proteins identified by yeast two-hybrid screening. The Bphi008a-interacting proteins were classified into five categories (as indicated in frame boxes) based on their putative functions. **B**. Yeast two-hybrid assay of the interaction between Bphi008a and OsbZIP60 or SDRP. TDO/3-AT plates containing 5 mM 3-AT (3-amino-1,2,4-Triazole); QDO/X-α-Gal/3-AT plates containing 10 mM 3-AT and 20 μg/ml X-α-Gal. **C**. Comparative expression levels of *OsbZIP60* after the BPH had been feeding for between 0 h and 96 h in WT and transgenic plants.